

Robust Fused Lasso Penalized Huber Regression with Nonasymptotic Property and Implementation Studies

Xin Xin^{1†}, Boyi Xie^{1†} and YunhaiXiao^{2*}

¹School of Mathematics and Statistics, Henan University, Kaifeng 475000, China.

^{2*}Center for Applied Mathematics of Henan Province, Henan University, Zhengzhou 450046, China.

*Corresponding author(s). E-mail(s): yhxiao@henu.edu.cn;
Contributing authors: xinxin@henu.edu.cn; byxiemath@163.com;

[†]These authors contributed equally to this work.

Abstract

For some special data in reality, such as the genetic data, adjacent genes may have the similar function. Thus ensuring the smoothness between adjacent genes is highly necessary. But, in this case, the standard lasso penalty just doesn't seem appropriate anymore. On the other hand, in high-dimensional statistics, some datasets are easily contaminated by outliers or contain variables with heavy-tailed distributions, which makes many conventional methods inadequate. To address both issues, in this paper, we propose an adaptive Huber regression for robust estimation and inference, in which, the fused lasso penalty is used to encourage the sparsity of the coefficients as well as the sparsity of their differences, i.e., local constancy of the coefficient profile. Theoretically, we establish its nonasymptotic estimation error bounds under ℓ_2 -norm in high-dimensional setting. The proposed estimation method is formulated as a convex, nonsmooth and separable optimization problem, hence, the alternating direction method of multipliers can be employed. In the end, we perform on simulation studies and real cancer data studies, which illustrate that the proposed estimation method is more robust and predictive.

Keywords: Adaptive Huber regression, fused lasso, nonasymptotic consistency, alternating direction method of multipliers, global convergence

1 Introduction

Data with ordered structures in many fields such as high-dimensional biomedical research [1], signal shapes [2], and air quality analysis [3], have emerged a series of new challenges both computationally and statistically. To deal with the ordered data, Tibshirani [4] proposed a novel fused lasso regression which imposed not only on the variable coefficients, like lasso, but also on the consecutive differences of variable coefficients based on the assumed order of feature variables. Since then, the

fused lasso has attained a lot of research activities. For instance, Petersen et al. [5] proposed a fused lasso additive model, in which each additive function is estimated to be piecewise constant. Mao et al. [6] incorporated temporal prior information to the missing traffic data and then used the fused lasso regularization to fit the temporal correlation of traffic data. Corsaro et al. [7] presented a model based on a fused lasso approach for the multi-period portfolio selection problem. Besides, the fused lasso is applied to portfolio weights, which

encourages sparse solutions and becomes a penalization on the difference of wealth allocated across the assets between rebalancing dates. Cui et al. [8] used a fused lasso framework to features reordering on the basis of their relevance with respect to the target feature. It enhanced the trade-off between the relevancy of each individual feature on the one hand and the redundancy between pairwise features on the other. Degras et al. [3] introduced a fused lasso for segmenting models with multivariate time series.

Associated with the characteristics of fused lasso, many estimation methods have been proposed, analyzed, and implemented. For the fused lasso penalized least square model of Tibshirani et al. [4], if the tuning parameters are fixed, the solution will correspond to a quadratic programming problem. Hence, a two-stage dynamic algorithm named SQOPT was specifically designed. This method transformed variables to the form of reduction between positive and negative parts because of the absolute value. However, the process of finding a solution is relatively complex and the computing time is also too long, especially when the variable dimension is large. Li et al. [9] focused on fused lasso model and applied a well-known linearized alternating direction method of multipliers (ADMM). But for large or even huge scale datasets, they believed that the customizing advanced operator splitting type methods may be more appropriate. Wang et al. [10] developed a new method of fused lasso with the adaptation of parameter ordering to scrutinize only adjacent-pair parameter's differences, which leads to a substantial reduction for the number of involved constraints. However, this method may be challenged by the increased computational complexity with respect to the underlying pattern of homogeneous parameters. Li et al. [1] proposed a highly efficient inexact semi-smooth Newton based augmented Lagrangian method for solving challenging large-scale fused lasso problems. But the Newton method usually requires more strict conditions on functions' properties.

Nevertheless, all these methods reviewed above ignored the case of the data being heavy-tailed. It was recently shown that, in this heavy-tailed case, using the Huber function loss instead of the least square is more appropriate. For example, Sun et al. [11] proposed an adaptive Huber

regression with an adaptive robustification parameter which has the ability to adopt the sample size, dimension, and moments of the random noise. We note that Huber loss function with a robust parameter is easily computed and its asymptotic properties have been well studied. For instance, Huang & Wu [12] adopted a pairwise Huber loss and then applied it in the situation when the noise only satisfies a weak moment condition. In their work, a comparison theorem to characterize the gap between the excess generalization error and the prediction error was established. Liu et al. [13] used a Huber loss function combining with a generalized lasso penalty to achieve robustness in estimation and variable selection. But they mainly focused on the formula of degrees of freedom that is used in information criteria for model selection.

On the numerical implementation progress, Sun et al. [11] solved the lasso penalized Huber regression by using the local iterative adaptive minimization algorithm of Fan et al. [14]. This method could control the accuracy and statistical error while fitting the high-dimensional model, but it could not handle the data with more complex structures. Meanwhile, Chen et al. [15] designed an accelerated proximal gradient algorithm to solve the matrix elastic-net regularized multivariate Huber regression model. Although this model could reduce the negative effect of outliers on estimators, it was not able to resistant the outliers well. Hence, other modified robust loss functions deserve further investigations. Luo et al. [16] proposed a robust distributed algorithm for fitting linear regressions when the data contains heavy-tailed or asymmetric errors with finite second moments. This procedure employed Barzilai-Borwein gradient descent and locally adaptive majorize-minimization, in low- and high-dimensional settings, respectively. Ghosh et al. [17] proposed a super-resolution algorithm using a Huber norm-based maximum likelihood estimation by combining with an adaptive directional Huber-Markov regularization. This algorithm is simple and can obtain solutions but the wide-angle image with high resolution are required.

Inspired by the aforementioned works, in this paper, we propose a novel fused lasso penalized adaptive Huber regression model. We show that this estimation method can not only deal with heavy-tailed problem, but also can guarantee the

smooth structures of the features. A nature question is: can this model give a good estimator which has a smooth and sparse property? To answer this question, we focus on an ADMM algorithm because of its widely applications in various fields, such as Xiao et al. [18], Jiao et al. [19]. We should emphasize that ADMM has been illustrated numerically that it is highly efficient for minimization problems with separable structures in both objective function and constraints. Another attractive feature is that the ADMM's convergence can be followed directly from some well-known convergence result according to the classical 2-block semi-proximal ADMM by Fazel et al. citefazel2013hankel.

Based on the issues mentioned above, this paper aims to handle the smoothness and outliers in multivariate linear regression, that is, we establish a fused lasso penalized adaptive Huber regression model. We show that this model possesses at least two advantages: (i) adjacent variables tend to be smooth, and (ii) the negative effect of outliers reduced. Besides, an efficient convergent ADMM algorithm is proposed. To the best of our knowledge, this is the first time to consider the case of dealing with smoothness and outliers in multivariate data set with heavy-tailed data.

The rest of the paper proceeds as follows. In Section 2, we quickly review the Huber loss and robustification parameter, followed by the proposal of fused lasso penalized adaptive Huber regression model. In Section 3, we sharply characterize the nonasymptotic performance of the proposed estimators in high dimension. We describe an implementation algorithm in Section 4. Subsequently, Section 5 and Section 6 are devoted to simulation studies and real data studies, respectively. In Section 7, we conclude this paper with some remarks.

Notation 1.1 For any multivariate $\mathbf{u} = (u_1, u_2, \dots, u_n)^\top \in \mathbb{R}^n$, we let $\|\mathbf{u}\|_p := (\sum_{i=1}^n |u_i|^p)^{1/p}$ be the ℓ_p -norm, and specially, $\|\mathbf{u}\|_\infty = \max_{1 \leq i \leq n} |u_i|$. For any two multivariate \mathbf{u} and \mathbf{v} , let $\langle \mathbf{u}, \mathbf{v} \rangle = \mathbf{u}^\top \mathbf{v}$, and $\mathbf{u} \odot \mathbf{v}$ be the Hadamard (entry-wise) product of \mathbf{u} and \mathbf{v} . For two sequences of real numbers $\{a_n\}_{n \geq 1}$ and $\{b_n\}_{n \geq 1}$, we use $a_n \lesssim b_n$ to denote $a_n \leq C_n b_n$ for a constant $C_n > 0$. For a linear map $\mathcal{A} : \mathbb{R}^p \rightarrow \mathbb{R}^q$, \mathcal{A}^* denotes its adjoint operator. Similarly, we denote the identity map by \mathcal{I} , or \mathbf{I} in matrix case.

2 Estimation Method

In this section, we begin with the linear regression model

$$\mathbf{y} = \mathbf{X}\boldsymbol{\beta} + \boldsymbol{\varepsilon}, \quad (1)$$

where $\mathbf{X} = (\mathbf{x}_1, \mathbf{x}_2, \dots, \mathbf{x}_p) \in \mathbb{R}^{n \times p}$ denotes a predictor matrix, $\mathbf{y} = (y_1, y_2, \dots, y_n)^\top \in \mathbb{R}^n$ be a response vector, $\boldsymbol{\beta} = (\beta_1, \beta_2, \dots, \beta_p)^\top \in \mathbb{R}^p$ be an unknown parameter vector, $\boldsymbol{\varepsilon} = (\varepsilon_1, \varepsilon_2, \dots, \varepsilon_n)^\top \in \mathbb{R}^n$ be a random error vector with ε_i being assumed independent and identically-distributed (i.i.d.) with mean 0 and variance σ_ε^2 , n be the sample size and p be the number of predictors. A common assumption is that the true coefficient vector $\boldsymbol{\beta}^*$ is sparse which guarantees the model identifiability and enhances the model fitting accuracy and interpretability.

As discussed previously, we will use a Huber loss function for a robust estimator of $\boldsymbol{\beta}$ in the model (1). First of all, we review an univariate Huber function for a given positive scalar $\tau > 0$, that is

$$h_\tau(x) = \begin{cases} \frac{1}{2}x^2, & \text{if } |x| \leq \tau, \\ \tau|x| - \frac{1}{2}\tau^2, & \text{if } |x| > \tau. \end{cases}$$

The scalar τ can be viewed as a shape parameter for controlling the amount of robustness. The Huber's criterion is similar to least square for a larger τ while it becomes more similar to LAD criterion for a smaller τ . In [20], Huber fixed $\tau = 1.345$ to get 95% efficiency at $\mathcal{N}(0, 1)$. In practice, an optimal τ can be determined by cross validation or on the basis of independent validation data sets.

For model (1), the multivariate Huber function is defined as the mean of the Huber function defined on component wise, that is,

$$\mathcal{L}_\tau(\mathbf{x}) = \frac{1}{n} \sum_{i=1}^n h_\tau(x_i).$$

By using this Huber function, we propose the following fused lasso penalized adaptive Huber regression model

$$\min_{\boldsymbol{\beta} \in \mathbb{R}^p} \mathcal{L}_\tau(\mathbf{y} - \mathbf{X}\boldsymbol{\beta}) + \lambda_1 \|\boldsymbol{\beta}\|_1 + \lambda_2 \sum_{j=2}^p |\beta_j - \beta_{j-1}|, \quad (2)$$

where $\lambda_1 > 0$ and $\lambda_2 > 0$ are tuning parameters. As usual, we call $\lambda_1 \|\boldsymbol{\beta}\|_1 + \lambda_2 \sum_{j=2}^p |\beta_j - \beta_{j-1}|$ the fused lasso penalty term. The most important merit of using fused lasso penalty term is that it has the ability to possess the smoothness property as well as variable selection. It is known that the ℓ_1 -norm is a convex relaxation of ℓ_0 -norm so that it can induce a sparse estimator. For convenience, we simplify the term $\sum_{j=2}^p |\beta_j - \beta_{j-1}|$ as $\|\mathbf{D}\boldsymbol{\beta}\|_1$, where

$$\mathbf{D} = \begin{bmatrix} -1 & 1 & 0 & \cdots & 0 \\ \vdots & \vdots & \ddots & \ddots & \vdots \\ 0 & -1 & \cdots & 1 & 0 \\ 0 & 0 & \cdots & -1 & 1 \end{bmatrix}$$

is named a difference operator matrix.

As we know, there are many efficient numerical approaches that can be employed to solve (2) in the special case that τ is sufficiently large, i.e., the least square loss case. However, numerical algorithms for this Huber loss in the form of (2) have never been investigated. Hence, developing an efficient and robust numerical algorithm for solving (2) becomes vitally important.

For the convenience of the later developments, we write (2) equivalently as the following model by using a triple of auxiliary variables, that is

$$\begin{aligned} \min_{z \in \mathbb{R}^n, \boldsymbol{\alpha}, \boldsymbol{\beta}, \boldsymbol{\gamma} \in \mathbb{R}^p} \quad & \mathcal{L}_\tau(\mathbf{y} - \mathbf{z}) + \lambda_1 \|\boldsymbol{\alpha}\|_1 + \lambda_2 \|\boldsymbol{\gamma}\|_1 \\ \text{s.t.} \quad & \begin{pmatrix} z \\ \boldsymbol{\alpha} \\ \boldsymbol{\gamma} \end{pmatrix} = \begin{pmatrix} \mathbf{X} \\ \mathbf{I} \\ \mathbf{D} \end{pmatrix} \boldsymbol{\beta}, \end{aligned} \quad (3)$$

where \mathbf{I} is a p -order identity matrix. For notational convenience, we then rewrite (3) as follows:

$$\begin{aligned} \min_{z \in \mathbb{R}^n, \boldsymbol{\alpha}, \boldsymbol{\beta}, \boldsymbol{\gamma} \in \mathbb{R}^p} \quad & \mathcal{L}_\tau(\mathbf{y} - \mathbf{z}) + \lambda_1 \|\boldsymbol{\alpha}\|_1 + \lambda_2 \|\boldsymbol{\gamma}\|_1 \\ \text{s.t.} \quad & \boldsymbol{\theta} = \tilde{\mathbf{X}}\boldsymbol{\beta}, \end{aligned} \quad (4)$$

where $\boldsymbol{\theta} := (z \ \boldsymbol{\alpha} \ \boldsymbol{\gamma})^\top$ and $\tilde{\mathbf{X}} := (\mathbf{X} \ \mathbf{I} \ \mathbf{D})^\top$. The implementation algorithm for solving (4) will be described in Section 4.

3 Statistical Theory

This section is devoted to the statistical theory of the estimation method (2). For convenience, we define an empirical loss function $\mathcal{L}_\tau(\boldsymbol{\beta}) :=$

$\frac{1}{n} \sum_{i=1}^n h_\tau(y_i - \mathbf{x}_i^\top \boldsymbol{\beta})$, and then denote

$$\hat{\boldsymbol{\beta}} \in \arg \min_{\boldsymbol{\beta} \in \mathbb{R}^p} \mathcal{L}_\tau(\boldsymbol{\beta}) + \lambda_1 \|\boldsymbol{\beta}\|_1 + \lambda_2 \sum_{j=2}^p |\beta_j - \beta_{j-1}|.$$

Besides, we use $\boldsymbol{\beta}^*$ to denote the ground truth. Let $\mathcal{S} := \text{supp}(\boldsymbol{\beta}^*) \subseteq \{1, 2, \dots, p\}$ be the true support set and let $|\mathcal{S}| = s$.

For characterizing the heavy-tailed random noise, we impose a bounded moment condition. Actually, this condition is a relaxation of the commonly used sub-Gaussian assumption described as follows:

Condition 3.1 (Bounded Moment Condition) *For $\delta > 0$, each element of the random error $\boldsymbol{\varepsilon}$ has a bounded $(1+\delta)$ -th moment, that is,*

$$v_\delta = \max_i \mathbb{E}(|\varepsilon_i|^{1+\delta}) < \infty.$$

Let $\mathbf{H}_\tau(\boldsymbol{\beta}) := \nabla^2 \mathcal{L}_\tau(\boldsymbol{\beta})$ be the Hessian matrix of the empirical loss function $\mathcal{L}_\tau(\boldsymbol{\beta})$. Let $\mathbf{S}_n = \frac{1}{n} \sum_{i=1}^n \mathbf{x}_i \mathbf{x}_i^\top$ be the empirical Gram matrix and it is assumed to be nonsingular throughout this paper. To establish the optimal statistical results in a general framework, we introduce a localized version of the restricted eigenvalue conditions which can be considered as a modification of Fan et al. [14].

Definition 1 (Localized Restricted Eigenvalue; LRE) The localized maximum and minimum eigenvalues of \mathbf{H}_τ is defined, respectively, as

$$\begin{aligned} & \kappa_+(m, c_0, r) \\ & := \sup_{\mathbf{u}, \boldsymbol{\beta}} \left\{ \frac{\langle \mathbf{u}, \mathbf{H}_\tau(\boldsymbol{\beta}) \mathbf{u} \rangle}{\|\mathbf{u}\|_2^2} : (\mathbf{u}, \boldsymbol{\beta}) \in \mathcal{C}(m, c_0, r) \right\}, \end{aligned}$$

and

$$\begin{aligned} & \kappa_-(m, c_0, r) \\ & := \inf_{\mathbf{u}, \boldsymbol{\beta}} \left\{ \frac{\langle \mathbf{u}, \mathbf{H}_\tau(\boldsymbol{\beta}) \mathbf{u} \rangle}{\|\mathbf{u}\|_2^2} : (\mathbf{u}, \boldsymbol{\beta}) \in \mathcal{C}(m, c_0, r) \right\}, \end{aligned}$$

where

$$\mathcal{C}(m, c_0, r) := \left\{ (\mathbf{u}, \boldsymbol{\beta}) \in \mathbb{R}^p \times \mathbb{R}^p : \forall J \subseteq \{1, \dots, p\} \right. \\ \left. \begin{array}{l} \text{such that } \mathcal{S} \subseteq J, |J| \leq m, \\ \|\mathbf{u}_{J^c}\|_1 \leq c_0 \|\mathbf{u}_J\|_1, \|\boldsymbol{\beta} - \boldsymbol{\beta}^*\|_1 \leq r \end{array} \right\}$$

is a local ℓ_1 cone.

Condition 3.2 $\mathbf{H}_\tau(\boldsymbol{\beta})$ satisfies the localized restricted eigenvalue condition $LRE(m, c_0, r)$, that is,

$$\kappa_{low} \leq \kappa_-(m, c_0, r) \leq \kappa_+(m, c_0, r) \leq \kappa_{up}$$

for some constants $\kappa_{low} > 0$ and $\kappa_{up} > 0$.

This condition is an unify to study generalized loss functions, whose Hessian may possibly depend on $\boldsymbol{\beta}$. Instead of \mathbf{H}_τ , in the following definition, we turn to the restricted eigenvalues of \mathbf{S}_n which is independent of $\boldsymbol{\beta}$.

Definition 2 (Restricted Eigenvalue; RE) The restricted maximum and minimum eigenvalues of \mathbf{S}_n are defined, respectively, as

$$\rho_+(m, c_0) := \sup_{\mathbf{u}} \left\{ \frac{\langle \mathbf{u}, \mathbf{S}_n \mathbf{u} \rangle}{\|\mathbf{u}\|_2^2} : \mathbf{u} \in \mathcal{C}(m, c_0) \right\},$$

and

$$\rho_-(m, c_0) := \inf_{\mathbf{u}} \left\{ \frac{\langle \mathbf{u}, \mathbf{S}_n \mathbf{u} \rangle}{\|\mathbf{u}\|_2^2} : \mathbf{u} \in \mathcal{C}(m, c_0) \right\},$$

where

$$\mathcal{C}(m, c_0) := \left\{ \mathbf{u} \in \mathbb{R}^p : \begin{array}{l} \forall J \subseteq \{1, \dots, p\} \text{ such that} \\ S \subseteq J, |J| \leq m, \|\mathbf{u}_{J^c}\|_1 \leq c_0 \|\mathbf{u}_J\|_1 \end{array} \right\}.$$

Condition 3.3 \mathbf{S}_n satisfies the restricted eigenvalue condition $RE(m, c_0)$, that is,

$$\kappa_{low} \leq \rho_-(m, c_0) \leq \rho_+(m, c_0) \leq \kappa_{up}$$

for some constants $\kappa_{low} > 0$ and $\kappa_{up} > 0$.

This condition is often used in high-dimensional nonasymptotic analysis. Furthermore, we can show that the localized restricted eigenvalues Condition 3.2 holds with high probability under the restricted eigenvalues Condition 3.3. The result reported in the following lemma shows that a proper bound for the localized restricted eigenvalues of \mathbf{H}_τ can be obtained with a high probability under some conditions on the robustification parameter τ and sample size n .

Lemma 3.1 Consider $\boldsymbol{\beta} \in \mathcal{C}(m, c_0, r)$ where $\mathcal{C}(m, c_0, r)$ is the local ℓ_1 cone defined in Definition 1. Let $\tau \geq \max\{8r, c_1(mv_\delta)^{1/(1+\delta)}\}$ and $n \geq c_2 m^2 t$ where $c_1, c_2 > 0$ are sufficient large constants only depending on c_0 and κ_{low} . Under Conditions 3.1 and 3.3, there exist constants κ_{low} and κ_{up} such that the localized restricted eigenvalue of $\mathbf{H}_\tau(\boldsymbol{\beta})$ satisfy

$$0 < \kappa_{low}/2 \leq \kappa_-(m, c_0, r) \leq \kappa_+(m, c_0, r) \leq \kappa_{up} < \infty$$

with probability at least $1 - e^{-t}$.

Definition 3 (Bregman Divergence) For convex loss function $\mathcal{L}_\tau(\cdot)$, the Bregman divergence between $\hat{\boldsymbol{\beta}}$ and $\boldsymbol{\beta}^*$ is defined as

$$D_{\mathcal{L}}(\hat{\boldsymbol{\beta}}, \boldsymbol{\beta}^*) := \mathcal{L}_\tau(\hat{\boldsymbol{\beta}}) - \mathcal{L}_\tau(\boldsymbol{\beta}^*) - \langle \nabla \mathcal{L}_\tau(\boldsymbol{\beta}^*), \hat{\boldsymbol{\beta}} - \boldsymbol{\beta}^* \rangle \geq 0.$$

Furthermore, it can define the following symmetric Bregman divergence between $\hat{\boldsymbol{\beta}}$ and $\boldsymbol{\beta}^*$ as

$$\begin{aligned} D_{\mathcal{L}}^s(\hat{\boldsymbol{\beta}}, \boldsymbol{\beta}^*) &:= D_{\mathcal{L}}(\hat{\boldsymbol{\beta}}, \boldsymbol{\beta}^*) + D_{\mathcal{L}}(\boldsymbol{\beta}^*, \hat{\boldsymbol{\beta}}) \\ &= \langle \nabla \mathcal{L}_\tau(\hat{\boldsymbol{\beta}}) - \nabla \mathcal{L}_\tau(\boldsymbol{\beta}^*), \hat{\boldsymbol{\beta}} - \boldsymbol{\beta}^* \rangle \geq 0. \end{aligned} \quad (5)$$

Lemma 3.2 Let $\boldsymbol{\beta}_l := \boldsymbol{\beta}^* + l(\boldsymbol{\beta} - \boldsymbol{\beta}^*)$ with $l \in (0, 1]$. For Huber loss function $\mathcal{L}_\tau(\cdot)$, it holds that

$$D_{\mathcal{L}}^s(\boldsymbol{\beta}_l, \boldsymbol{\beta}^*) \leq l D_{\mathcal{L}}^s(\boldsymbol{\beta}, \boldsymbol{\beta}^*).$$

Lemma 3.3 (Restricted Strong Convexity) Under the condition in Lemma 3.1, for any $(\mathbf{u}, \boldsymbol{\beta}) \in \mathcal{C}(m, c_0, r)$, we have

$$D_{\mathcal{L}}^s(\boldsymbol{\beta}, \boldsymbol{\beta}^*) \geq \frac{\kappa_{low}}{2} \|\boldsymbol{\beta} - \boldsymbol{\beta}^*\|_2^2$$

with probability at least $1 - e^{-t}$.

Lemma 3.4 (ℓ_1 cone property) Assume that $\|\nabla \mathcal{L}_\tau(\boldsymbol{\beta}^*)\|_\infty \leq \lambda_1/2$ and $\|\mathbf{D}\|_\infty = d > 0$. Let $\lambda_2 = b\lambda_1$ with $b > 0$. Let $\hat{\boldsymbol{\beta}}$ be an optimal solution of (2). We have that $\hat{\boldsymbol{\beta}}$ falls in a local ℓ_1 cone, where

$$\|(\hat{\boldsymbol{\beta}} - \boldsymbol{\beta}^*)_{S^c}\|_1 \leq \frac{2bd + 3}{2bd + 1} \|(\hat{\boldsymbol{\beta}} - \boldsymbol{\beta}^*)_S\|_1.$$

For a similar proof of this lemma, one may refer to Fan et al. [14]. This lemma shows that the optimal solution $\hat{\boldsymbol{\beta}}$ of (2) must falls into a ℓ_1 cone.

In light of above analysis, we are ready to present the main results on the regularized adaptive Huber estimator in high dimension.

Theorem 1 Let $\hat{\boldsymbol{\beta}}$ be the fused lasso regularized Huber estimator to (2). For any $t > 0$ and $\tau_0 \geq \nu_\delta := \min\{v_\delta^{1/(1+\delta)}, v_1^{1/2}\}$, let the robust and regularized parameters be

$$\begin{aligned} \tau &= \tau_0(n/t)^{\max\{1/(1+\delta), 1/2\}}, \\ \lambda_1 &\geq 4\tau_0(t/n)^{\min\{\delta/(1+\delta), 1/2\}}. \end{aligned}$$

Assume that Condition 3.1, 3.2 and 3.3 hold with $c_0 = \frac{2bd+3}{2bd+1}$, $b > 0$, $d > 0$ and $r \gtrsim \lambda_1 \kappa_{low}^{-1} s$. Then we have

$$\|\hat{\boldsymbol{\beta}} - \boldsymbol{\beta}^*\|_2 \leq \lambda_1 \kappa_{low}^{-1} \sqrt{s}$$

with probability at least $1 - (1 + 2p)e^{-t}$ as long as $n \geq c_3 m^2 t$ for a certain large constant $c_3 > 0$.

Theorem 1 builds the nonasymptotics convergence rates of our proposed estimation method in the high-dimensional setting. Thus, the upper bound in Theorem 1 can be rewritten as

$$\|\hat{\boldsymbol{\beta}} - \boldsymbol{\beta}^*\|_2 \lesssim \sqrt{\frac{p_{\text{eff}}}{n_{\text{eff}}}}$$

by setting the effective dimension as $p_{\text{eff}} := s$ and the effective sample size as $n_{\text{eff}} := (n/t)^{\min\{2\delta/(1+\delta), 1\}}$. The effective dimension depends only on the sparsity while the effective sample size depends only on the sample size divided by the probability parameter. We can observe that the rate of convergence is affected by the heavy-tailedness only through the effective sample size because the effective dimension keeps the same regardless of δ .

4 Numerical Algorithm

4.1 Preliminary Results in Convex Analysis

Now we quickly review some useful results in convex analysis [21] for subsequent developments. Let $f : \mathbb{R}^p \rightarrow (-\infty, +\infty]$ be a proper closed convex function. The conjugate function of f at \mathbf{y} is defined as $f^*(\mathbf{y}) := \sup_{\mathbf{x}} \{\langle \mathbf{x}, \mathbf{y} \rangle - f(\mathbf{x})\}$. It is well known that $f^*(\mathbf{y})$ is convex and closed, proper if and only if f is proper. The proximal mapping of \mathbf{x} associates to f is defined by

$$\mathcal{P}_{f(\cdot)}^c(\mathbf{y}) = \arg \min_{\mathbf{x}} \{f(\mathbf{x}) + \frac{1}{2c} \|\mathbf{x} - \mathbf{y}\|_2^2\},$$

where $c > 0$ is a positive scalar. The proximal mapping $\mathcal{P}_{f(\cdot)}^c(\mathbf{y})$ exists and is unique for all \mathbf{y} if f is proper closed and convex. For any $\mathbf{y} \in \mathbb{R}^p$, the Moreau's identity is

$$\mathbf{y} = \mathcal{P}_{f(\cdot)}^c(\mathbf{y}) + c\mathcal{P}_{f^*(\cdot)}^{1/c}(\mathbf{y}/c),$$

which means that the proximal mapping of f^* can be attained via computing the proximal mapping associated to f . For example, the proximal mapping of an ℓ_1 -norm function is defined as

$$\mathcal{P}_{\|\cdot\|_1}^c(\mathbf{y}) = \arg \min_{\mathbf{x}} \{\|\mathbf{x}\|_1 + \frac{1}{2c} (\mathbf{x} - \mathbf{y})^2\},$$

which has a unique explicit solution, that is

$$\mathcal{P}_{\|\cdot\|_1}^c(\mathbf{y}) = \text{sgn}(\mathbf{y}) \odot \max\{|\mathbf{y}| - c, 0\}, \quad (6)$$

where ‘sgn’ is a sign function and the symbol \odot is Hadamard product of a pair of vectors.

Consider the following convex composite programming problem

$$\begin{aligned} \min_{\mathbf{x}, \mathbf{y}} \quad & f(\mathbf{x}) + g(\mathbf{y}) \\ \text{s.t.} \quad & \mathbf{A}\mathbf{x} + \mathbf{B}\mathbf{y} = \mathbf{c}, \end{aligned} \quad (7)$$

where $f(\cdot)$ and $g(\cdot)$ are proper closed convex functions, $\mathbf{A} \in \mathbb{R}^{l \times p}$ and $\mathbf{B} \in \mathbb{R}^{l \times q}$ are matrices, $\mathbf{c} \in \mathbb{R}^l$ is a given data. The Lagrangian function of (7) as

$$\mathcal{L}(\mathbf{x}, \mathbf{y}; \mathbf{z}) = f(\mathbf{x}) + g(\mathbf{y}) - \langle \mathbf{z}, \mathbf{A}\mathbf{x} + \mathbf{B}\mathbf{y} - \mathbf{c} \rangle, \quad (8)$$

where $\mathbf{z} \in \mathbb{R}^n$ often referred to as the Lagrangian dual variable. Theoretically, the Lagrange dual function is defined as minimizing $\mathcal{L}(\mathbf{x}, \mathbf{y}; \mathbf{z})$ on (\mathbf{x}, \mathbf{y}) , and the Lagrange dual problem of (7) is defined as maximizing the Lagrange dual function on \mathbf{z} , that is,

$$\max_{\mathbf{z}} -f^*(\mathbf{A}^\top \mathbf{z}) - g^*(\mathbf{B}^\top \mathbf{z}) + \langle \mathbf{z}, \mathbf{c} \rangle. \quad (9)$$

To ensure (7) along with its dual form (9) have optimal solutions, throughout this section, we make the following assumptions :

Assumption 4.1 (i) The functions $f : \mathbb{R}^p \rightarrow \mathbb{R} \cup \{+\infty\}$ and $g : \mathbb{R}^q \rightarrow \mathbb{R} \cup \{+\infty\}$ in (7) are closed, proper, and convex; (ii) the Lagrangian function has a saddle point (i.e., there exist $(\mathbf{x}^*, \mathbf{y}^*, \mathbf{z}^*)$ for which $\mathcal{L}(\mathbf{x}^*, \mathbf{y}^*, \mathbf{z}) \leq \mathcal{L}(\mathbf{x}^*, \mathbf{y}^*, \mathbf{z}^*) \leq \mathcal{L}(\mathbf{x}, \mathbf{y}, \mathbf{z}^*)$ holds for all $(\mathbf{x}, \mathbf{y}, \mathbf{z})$).

Note that the second part of this assumption is equivalent to a strong duality, which can be ensured by constraint qualifications such as Slater's condition [21]. For more details on constraints qualifications in optimization, we refer the readers to [22].

4.2 Optimality Conditions and Algorithm

In this part, we use ADMM to solve fused lasso regularized adaptive Huber regression problem

(4). Let $\boldsymbol{\mu} := (\boldsymbol{\mu}_z \ \boldsymbol{\mu}_\alpha \ \boldsymbol{\mu}_\gamma)^\top \in \mathbb{R}^{n+2p-1}$ be multiplier associate to the constraint in (4), then the Lagrangian function takes the following form

$$\begin{aligned} & \mathcal{L}(z, \boldsymbol{\alpha}, \boldsymbol{\beta}, \boldsymbol{\gamma}; \boldsymbol{\mu}) \\ & = \mathcal{L}_\tau(\mathbf{y} - z) + \lambda_1 \|\boldsymbol{\alpha}\|_1 + \lambda_2 \|\boldsymbol{\gamma}\|_1 + \boldsymbol{\mu}^\top (\boldsymbol{\theta} - \tilde{\mathbf{X}}\boldsymbol{\beta}). \end{aligned} \quad (10)$$

From optimization theory, it is known that finding a saddle point $(\bar{z}, \bar{\boldsymbol{\alpha}}, \bar{\boldsymbol{\beta}}, \bar{\boldsymbol{\gamma}}; \bar{\boldsymbol{\mu}})$ of (10) is equivalent to finding $(\bar{z}, \bar{\boldsymbol{\alpha}}, \bar{\boldsymbol{\beta}}, \bar{\boldsymbol{\gamma}}; \bar{\boldsymbol{\mu}})$ such that the following Karush-Kuhn-Tucker (KKT) system is satisfied

$$\begin{cases} -\partial \mathcal{L}_\tau(\mathbf{y} - \bar{z}) + \bar{\boldsymbol{\mu}}_z \ni 0, \\ \lambda_1 \partial \|\bar{\boldsymbol{\alpha}}\|_1 + \bar{\boldsymbol{\mu}}_\alpha \ni 0, \\ \tilde{\mathbf{X}}^\top \bar{\boldsymbol{\mu}} = 0, \\ \lambda_2 \partial \|\bar{\boldsymbol{\gamma}}\|_1 + \bar{\boldsymbol{\mu}}_\gamma \ni 0, \\ \bar{\boldsymbol{\theta}} - \tilde{\mathbf{X}}\bar{\boldsymbol{\beta}} = 0, \end{cases} \quad (11)$$

where $(\bar{z}, \bar{\boldsymbol{\alpha}}, \bar{\boldsymbol{\beta}}, \bar{\boldsymbol{\gamma}})$ is an optimal solution of (4) and $\bar{\boldsymbol{\mu}}$ is an optimal solution of the corresponding dual problem. We note that the KKT system plays a key role in the stopping criteria for the algorithm given below.

Let $\sigma > 0$ be a penalty parameter. The augmented Lagrangian function to problem (4) is given as

$$\begin{aligned} & \mathcal{L}_\sigma(z, \boldsymbol{\alpha}, \boldsymbol{\beta}, \boldsymbol{\gamma}; \boldsymbol{\mu}) \\ & := \mathcal{L}_\tau(\mathbf{y} - z) + \lambda_1 \|\boldsymbol{\alpha}\|_1 + \lambda_2 \|\boldsymbol{\gamma}\|_1 + \boldsymbol{\mu}^\top (\boldsymbol{\theta} - \tilde{\mathbf{X}}\boldsymbol{\beta}) \\ & \quad + \frac{\sigma}{2} \|\boldsymbol{\theta} - \tilde{\mathbf{X}}\boldsymbol{\beta}\|_2^2, \end{aligned}$$

or equivalently,

$$\begin{aligned} \mathcal{L}_\sigma(z, \boldsymbol{\alpha}, \boldsymbol{\beta}, \boldsymbol{\gamma}; \boldsymbol{\mu}) & = \mathcal{L}_\tau(\mathbf{y} - z) + \lambda_1 \|\boldsymbol{\alpha}\|_1 + \lambda_2 \|\boldsymbol{\gamma}\|_1 \\ & \quad + \frac{\sigma}{2} \|\boldsymbol{\theta} - \tilde{\mathbf{X}}\boldsymbol{\beta} + \boldsymbol{\mu}/\sigma\|_2^2. \end{aligned} \quad (12)$$

Noting that there are four blocks involved in problem (4) and each block is completely independent of each other, then the ADMM reviewed before can be used directly. For convenience, we view $\boldsymbol{\beta}$ as a group and $(\boldsymbol{\alpha}, \boldsymbol{\gamma}, z)$ as another. Given an initial point, then the ADMM reduces the following iterative framework:

$$\boldsymbol{\beta}^{k+1} = \arg \min_{\boldsymbol{\beta}} \mathcal{L}_\sigma(z^k, \boldsymbol{\alpha}^k, \boldsymbol{\beta}, \boldsymbol{\gamma}^k; \boldsymbol{\mu}^k), \quad (13)$$

$$\boldsymbol{\theta}^{k+1} := (\boldsymbol{\alpha}^{k+1}, \boldsymbol{\gamma}^{k+1}, z^{k+1})$$

$$= \arg \min_{\boldsymbol{\alpha}, \boldsymbol{\gamma}, z} \mathcal{L}_\sigma(z, \boldsymbol{\alpha}, \boldsymbol{\beta}^{k+1}, \boldsymbol{\gamma}; \boldsymbol{\mu}^k), \quad (14)$$

$$\boldsymbol{\mu}^{k+1} = \boldsymbol{\mu}^k + \pi \sigma (\boldsymbol{\theta}^{k+1} - \tilde{\mathbf{X}}\boldsymbol{\beta}^{k+1}), \quad (15)$$

where $\pi \in (0, (1 + \sqrt{5})/2)$ is a step length. Clearly, the main computational cost lies in the subproblems with respect to variables $z, \boldsymbol{\alpha}, \boldsymbol{\beta}$ and $\boldsymbol{\gamma}$. In the following, we show that each subproblem admits closed form solutions which make this iterative framework is easily implemented.

4.3 Subproblems' Solving

This part is devoted to solving the $\boldsymbol{\beta}$ -subproblem and the $(\boldsymbol{\alpha}, \boldsymbol{\gamma}, z)$ -subproblem involved in (13) and (14), respectively.

With fixed values of other variables, the $\boldsymbol{\beta}$ -subproblem takes the following form

$$\begin{aligned} \boldsymbol{\beta}^{k+1} & = \arg \min_{\boldsymbol{\beta}} \mathcal{L}_\sigma(z^k, \boldsymbol{\alpha}^k, \boldsymbol{\beta}, \boldsymbol{\gamma}^k; \boldsymbol{\mu}^k) \\ & = \arg \min_{\boldsymbol{\beta}} -\langle \boldsymbol{\mu}^k, \tilde{\mathbf{X}}\boldsymbol{\beta} \rangle + \frac{\sigma}{2} \|\boldsymbol{\theta}^k - \tilde{\mathbf{X}}\boldsymbol{\beta}\|_2^2. \end{aligned}$$

Noting that it is actually a quadratic programming, then, its solution can be easily derived with the following compact form

$$\boldsymbol{\beta}^{k+1} = (\tilde{\mathbf{X}}^\top \tilde{\mathbf{X}})^{-1} \tilde{\mathbf{X}}^\top (\boldsymbol{\theta}^k + \boldsymbol{\mu}^k/\sigma). \quad (16)$$

For the $(\boldsymbol{\alpha}, \boldsymbol{\gamma}, z)$ -subproblem, we notice that the variable $\boldsymbol{\alpha}, \boldsymbol{\gamma}$, and z are independent of each other, which means that finding them together is equivalent to finding them one by one with an arbitrary order. Firstly, when $z := z^k$ and $\boldsymbol{\gamma} := \boldsymbol{\gamma}^k$ are fixed, the $\boldsymbol{\alpha}$ -subproblem can be expressed as

$$\begin{aligned} & \boldsymbol{\alpha}^{k+1} \\ & = \arg \min_{\boldsymbol{\alpha}} \mathcal{L}_\sigma(z^k, \boldsymbol{\alpha}, \boldsymbol{\beta}^{k+1}, \boldsymbol{\gamma}^k; \boldsymbol{\mu}^k) \\ & = \arg \min_{\boldsymbol{\alpha}} \left\{ \lambda_1 \|\boldsymbol{\alpha}\|_1 + \frac{\sigma}{2} \|\boldsymbol{\alpha} - \boldsymbol{\beta}^{k+1} + \boldsymbol{\mu}_\alpha^k/\sigma\|_2^2 \right\}, \end{aligned}$$

which admits closed form solutions by using (6), that is,

$$\boldsymbol{\alpha}^{k+1} = \text{sgn}(\boldsymbol{\xi}^k) \odot \max\{|\boldsymbol{\xi}^k| - \lambda_1/\sigma, 0\}, \quad (17)$$

where $\boldsymbol{\xi}^k = \boldsymbol{\beta}^{k+1} - \boldsymbol{\mu}_\alpha^k/\sigma$. Secondly, when $z := z^k$ and $\boldsymbol{\alpha} := \boldsymbol{\alpha}^{k+1}$ are fixed, the $\boldsymbol{\gamma}$ -subproblem takes

the following form

$$\begin{aligned} & \gamma^{k+1} \\ &= \arg \min_{\gamma} \mathcal{L}_{\sigma}(\mathbf{z}^k, \boldsymbol{\alpha}^{k+1}, \boldsymbol{\beta}^{k+1}, \gamma; \boldsymbol{\mu}^k) \\ &= \arg \min_{\gamma} \left\{ \lambda_2 \|\boldsymbol{\gamma}\|_1 + \frac{\sigma}{2} \|\boldsymbol{\gamma} - \mathbf{D}\boldsymbol{\beta}^{k+1} + \boldsymbol{\mu}_{\gamma}^k/\sigma\|_2^2 \right\}, \end{aligned}$$

which also admits closed form solutions from (6), that is,

$$\boldsymbol{\gamma}^{k+1} = \text{sgn}(\boldsymbol{\eta}^k) \odot \max\{|\boldsymbol{\eta}^k| - \lambda_2/\sigma, 0\}, \quad (18)$$

where $\boldsymbol{\eta}^k = \mathbf{D}\boldsymbol{\beta}^{k+1} - \boldsymbol{\mu}_{\gamma}^k/\sigma$. Thirdly, when $\boldsymbol{\gamma} := \boldsymbol{\gamma}^{k+1}$ and $\boldsymbol{\alpha} := \boldsymbol{\alpha}^{k+1}$ are fixed, the \mathbf{z} -subproblem can be computed element-wise regarding to n independent one-dimensional problems, that is,

$$\begin{aligned} & \mathbf{z}^{k+1} \\ &= \arg \min_{\mathbf{z}} \mathcal{L}_{\sigma}(\mathbf{z}, \boldsymbol{\alpha}^{k+1}, \boldsymbol{\beta}^{k+1}, \boldsymbol{\gamma}^{k+1}; \boldsymbol{\mu}^k) \\ &= \arg \min_{\mathbf{z}} \left\{ \mathcal{L}_{\tau}(\mathbf{y} - \mathbf{z}) + \frac{\sigma}{2} \|\mathbf{z} - \mathbf{X}\boldsymbol{\beta}^{k+1} + \boldsymbol{\mu}_{\mathbf{z}}^k/\sigma\|_2^2 \right\} \\ &= \sum_{i=1}^n \arg \min_{z_i} \left\{ \frac{1}{n} h_{\tau}(y_i - z_i) \right. \\ & \quad \left. + \frac{\sigma}{2} (z_i - \mathbf{x}_i \boldsymbol{\beta}^{k+1} + \mu_{z_i}^k/\sigma)^2 \right\}. \end{aligned}$$

We observe that solving each z_i -subproblem

$$\arg \min_{z_i} \frac{1}{n} h_{\tau}(y_i - z_i) + \frac{\sigma}{2} (z_i - \mathbf{x}_i \boldsymbol{\beta}^{k+1} + \mu_{z_i}^k/\sigma)^2, \quad (19)$$

can be divided into the following two cases:

Case 1: In the case of $|y_i - z_i| \leq \tau$, (19) reduces to

$$\arg \min_{z_i} \frac{1}{2n} (y_i - z_i)^2 + \frac{\sigma}{2} (z_i - \mathbf{x}_i \boldsymbol{\beta}^{k+1} + \mu_{z_i}^k/\sigma)^2.$$

Then, its solution takes the following form

$$z_i^{k+1} = (y_i + n\sigma \mathbf{x}_i \boldsymbol{\beta}^{k+1} - n\mu_{z_i}^k)/(n\sigma + 1). \quad (20)$$

Case 2: In the case of $|y_i - z_i| > \tau$, (19) reduces to

$$\arg \min_{z_i} \frac{\tau}{n} |y_i - z_i| + \frac{\sigma}{2} (z_i - \mathbf{x}_i \boldsymbol{\beta}^{k+1} + \mu_{z_i}^k/\sigma)^2.$$

Let $h_i = y_i - z_i$, then it becomes

$$\arg \min_{z_i} \frac{\tau}{n} |h_i| + \frac{\sigma}{2} (h_i - y_i + \mathbf{x}_i \boldsymbol{\beta}^{k+1} - \mu_{z_i}^k/\sigma)^2,$$

which admits closed form solutions by using (6), that is,

$$h_i^{k+1} = \text{sgn}(\zeta_i^k) \cdot \max\{|\zeta_i^k| - \tau/(n\sigma), 0\},$$

where $\zeta_i^k = y_i - \mathbf{x}_i \boldsymbol{\beta}^{k+1} + \mu_{z_i}^k/\sigma$. Therefore,

$$\begin{aligned} z_i^{k+1} &= y_i - h_i^{k+1} \\ &= y_i - \text{sgn}(\zeta_i^k) \odot \max\{|\zeta_i^k| - \tau/(n\sigma), 0\}. \end{aligned} \quad (21)$$

In light of above analysis, we are ready to state the iterative framework of ADMM, named FHADMM, for solving the fused lasso penalized adaptive Huber regression problem (4) as follows.

Algorithm 1 FHADMM

Input: Choose the robustification parameter $\tau > 0$, the regularization parameters $\lambda_1, \lambda_2 > 0$, the penalty parameter $\sigma > 0$ and step length $\pi \in (0, (1 + \sqrt{5})/2)$. Choose an initial point $\mathbf{z}^0 \in \mathbb{R}^n$, $\boldsymbol{\alpha}^0 \in \mathbb{R}^p$, $\boldsymbol{\gamma}^0 \in \mathbb{R}^{p-1}$ and initial multipliers $\boldsymbol{\mu}^0 = (\boldsymbol{\mu}_{\mathbf{z}}^0 \ \boldsymbol{\mu}_{\boldsymbol{\alpha}}^0 \ \boldsymbol{\mu}_{\boldsymbol{\gamma}}^0)^{\top} \in \mathbb{R}^{n+2p-1}$. For $k = 0, 1, 2, \dots$, do the following steps iteratively.

Output: Iterate until a certain ‘stopping criterion’ is met:

- 1: update $\boldsymbol{\beta}^{k+1}$ by (16);
- 2: update $\boldsymbol{\alpha}^{k+1}$ by (17);
- 3: update $\boldsymbol{\gamma}^{k+1}$ by (18);
- 4: update \mathbf{z}^{k+1} by (21);
- 5: update $\boldsymbol{\mu}^{k+1}$ by

$$\begin{aligned} \boldsymbol{\mu}_{\mathbf{z}}^{k+1} &= \boldsymbol{\mu}_{\mathbf{z}}^k + \pi\sigma(\mathbf{z}^{k+1} - \mathbf{X}\boldsymbol{\beta}^{k+1}); \\ \boldsymbol{\mu}_{\boldsymbol{\alpha}}^{k+1} &= \boldsymbol{\mu}_{\boldsymbol{\alpha}}^k + \pi\sigma(\boldsymbol{\alpha}^{k+1} - \boldsymbol{\beta}^{k+1}); \\ \boldsymbol{\mu}_{\boldsymbol{\gamma}}^{k+1} &= \boldsymbol{\mu}_{\boldsymbol{\gamma}}^k + \pi\sigma(\boldsymbol{\gamma}^{k+1} - \mathbf{D}\boldsymbol{\beta}^{k+1}); \end{aligned}$$

return $\boldsymbol{\beta}^{k+1}$.

In the experiment part, we fix the penalty parameter as $\sigma = 0.1$ for simplicity. Certainly, other techniques can be used so as to setting this value dynamically, e.g., Boyd et al. [23]. Besides, we use an unit step length, i.e., $\pi = 1$, because of

its extensive using in the algorithms for statistics learning. On the other hand, the convergence in the unit steplength case can be followed directly in the existing literature, such as Fazel et al. [24] and Yang & Han [25]. To make this part is easier to follow, we state its convergence result without proof because FHADMM is actually a standard ADMM with blocks β and (α, γ, z) . In summary, the convergence result of FHADMM can be described as follows.

Theorem 2 *Let $\{(z^k, \alpha^k, \beta^k, \gamma^k)\}$ be generated by FHADMM. If $\pi \in (0, (1 + \sqrt{5})/2)$, then the sequence $\{(z^k, \alpha^k, \beta^k, \gamma^k)\}$ converges to an optimal solution $(\hat{z}, \hat{\alpha}, \hat{\beta}, \hat{\gamma})$ to (3) and $\{(\mu_z^k, \mu_\alpha^k, \mu_\gamma^k)\}$ converges to an optimal solution $\hat{\mu}$ to the dual problem of (3).*

Proof See [24, Theorem B1]. \square

At the end of this section, we state the stopping condition of Algorithm FHADMM. According to (11), we use the KKT residuals to measure the quality of the derived solution, i.e.,

$$Res := \max\{\phi_\mu, \phi_z, \phi_\alpha, \phi_\beta, \phi_\gamma\} < Tol,$$

where

$$\begin{aligned}\phi_\mu &:= \|\theta - \tilde{X}\beta\|, \\ \phi_z &:= \frac{\|\mathbf{y} - z - \mathcal{P}_{\mathcal{L}_\tau}(\mathbf{y} - z - \mu_z)\|}{1 + \|\mathbf{y} - z\| + \|\mu_z\|}, \\ \phi_\alpha &:= \frac{\|\alpha - \mathcal{P}_{\|\cdot\|_1}(\alpha - \mu_\alpha/\lambda_1)\|}{1 + \|\alpha\| + \|\mu_\alpha/\lambda_1\|}, \\ \phi_\beta &:= \|\tilde{X}\mu\|, \\ \phi_\gamma &:= \frac{\|\gamma - \mathcal{P}_{\|\cdot\|_1}(\gamma - \mu_\gamma/\lambda_2)\|}{1 + \|\gamma\| + \|\mu_\gamma/\lambda_2\|},\end{aligned}$$

and ‘Tol’ is a small error tolerance. In our experiments, we set $Tol = 10^{-3}$ which is illustrated to be enough to derive better quality estimations in experimental preparations. Besides, if this stopping criterion can not meet within 2000 number of iterations, we also force the iterative process of FHADMM terminate. In this case, we say this algorithm fails to the corresponding problem.

5 Numerical Studies on Synthetic Data

In this section, we present some numerical studies by using a typical synthetic data to evaluate the performance of our proposal model in both low and high dimensions. All runs are performed on a laptop with Intel(R) Core(TM) i7 – 9750 CPU (2.59 GHz) and 8 GB RAM.

For all of our numerical studies, n denotes training set size, n_{test} denotes test set size and p denotes the number of features, or problem’s dimension. Each row of X is generated by a normal distribution with mean zero and covariance matrix Σ , where $\Sigma_{ij} = 0.5^{|i-j|}$ for $1 \leq i, j \leq p$. We simulate data with sparse and smooth vector $\beta^* := (\beta_1^*, \beta_2^*)$, where $\beta_1^* := (1, 1, 1, 1, 1, 1, 2, 1.5, 1.5, 1.5, 1.5)$ and $\beta_2^* := (0, 0, \dots, 0)$ is a zero vector which the number of zero element is $p - 12$. In this part, we consider the case of $p = 50, 200$, and 400.

The response variable \mathbf{y} is generated according to $\mathbf{y} = \mathbf{X}\beta^* + \varepsilon$. We consider three different distributions of random noise $\varepsilon \in \mathbb{R}^n$:

- (i) The normal distribution $\mathcal{N}(0, 0.05^2)$;
- (ii) The t distribution with degrees of freedom 1.5;
- (iii) The lognormal distribution $\log \mathcal{N}(0, 2^2)$.

We note that performing the algorithm FHADMM involves a robustification parameter τ and a couple of regularization parameters λ_1 and λ_2 . For τ , its traditional choice is 1.345. Here, to get a better estimation, we choose it dynamically as $\tau = a\sqrt{n/\log(p)}$ with $a = \{0.4, 0.45, \dots, 1.45, 1.5\}$. There are many techniques on the choice of λ_1 and λ_2 , such as [26] and [27]. Here we choose them by minimizing the estimation errors and prediction errors simultaneously. More details are ignored here because they beyond the scope of this paper.

In this part, we also do comparisons with other two typical estimation methods:

- (i) The efficient fused lasso algorithm (EFLA): This algorithm was proposed by Liu et al. [28] which is used for a fused lasso penalized least squares estimation. One key building block in EFLA is the Fused Lasso Signal Approximator (FLSA). The package of this algorithm is available at the website: <https://github.com/jaredhuling/fusedlasso>. Here, we name it as ‘EFLA’.

(ii) The `fusedlasso` package proposed by Tibshirani & Taylor [29]. This solver aims to a fused lasso regularized least squares model via a dual path algorithm. Here, we name it as “FLDP”.

To evaluate the performance of each method, we measure the accuracy by the using of the Mean Squared Errors (MSE), which is defined as the difference between the estimated regression coefficients $\hat{\beta}$ and the truth β^* under an ℓ_2 -norm. To visibly observe the performance of each method, we report the estimated coefficient $\hat{\beta}$ vs. the ground truth β^* in Figure 1, Figure 2, and Figure 3 in the sense that the normal distribution, the t distribution, and the lognormal distribution on the noise ε are considered, respectively. Moreover, in each distribution case, we also consider three different dimensions, say $p = 50, 200, \text{ and } 400$, and report the results row by row in each figure. The methods used in each test case are EFLA, FLDP, and FHADMM, and the results according to each method are listed column by column at each figure.

To compare each method in a relatively fair way, we run the code 200 times and record the average mean (MSE), the average standard error of the residuals (std), and the average computing time (CPU). The detailed numerical results are reported in Table 1 in which the results for best performance are marked in bold. It should be noted that the first column in Table 1 denotes the type of distribution of noise, and the second column denotes the names we concerned where the subscribe represents its dimension. From this table, we can derive the following conclusions:

(i) Our proposed method FHADMM has better performance for t distribution and lognormal distribution, and is competitive with EFLA and FLDP for normal distribution, which means that our method performs better if heavy tailed noise contained. We think this is not surprising because the least square model is widely known to have strong theoretical guarantees under Gaussian noise. We also see that, under different distribution cases, FHADMM performs a little better when $p = 400$, which indicates that our proposed method is more suitable for solving higher dimensional problems. And particularly, under the lognormal distribution, our proposed method is a winner, which indicates that in the case of the data being not following symmetrical distribution and having long tails, our method is the best choice.

(ii) From the standard error of residual ‘std’, we see that the values derived by our estimation method are always lower, and they are more stable in the sense that they changes slightly at each test case. For each method, we also see that when the samples contain more outliers, the values of the standard error of residual may increase at each noise case.

(iii) When turning our attention to the computing time, we see that our method requires the least time at the most test cases. We note that FLDP is the slowest especially in the high-dimensional case. The reason lies in that a matrix computation is needed at each iteration, which may takes the main computing burden. In contrast, EFLA seems a little better because a Nesterov’s method is employed to produce an approximation solution per-iteration. In summary, the series of experiments demonstrate that our proposed method is the faster and highly efficient to estimate the coefficient in the heavily tailed data case.

Table 1 The MSE, std and CPU results of EFLA, FLDP, and FHADMM methods

		EFLA	FLDP	FHADMM	
\mathcal{N}	MSE ₅₀	0.201	5.555e-6	0.112	
	std ₅₀	1.595	7.798e-6	0.046	
	CPU ₅₀	0.019	1.230	0.049	
	MSE ₂₀₀	1.367e-6	16.901	0.917	
	std ₂₀₀	47.579	1.735e+2	0.122	
	CPU ₂₀₀	0.083	26.488	0.199	
	MSE ₄₀₀	1.334	1.223e-5	2.562	
	std ₄₀₀	8.038	1.814e-5	0.752	
	CPU ₄₀₀	0.400	98.026	0.315	
	t	MSE ₅₀	1.195	57.713	7.256
		std ₅₀	5.219e+3	4.756e+4	3.318
		CPU ₅₀	0.009	1.249	0.057
MSE ₂₀₀		0.290	2.838e+4	21.336	
std ₂₀₀		2.443e+4	1.767e+5	4.890	
CPU ₂₀₀		0.265	30.312	0.106	
MSE ₄₀₀		4.068e+4	82.909	29.312	
std ₄₀₀		5.625e+5	7.336e+2	4.764	
CPU ₄₀₀		0.599	134.291	0.282	
$\log \mathcal{N}$		MSE ₅₀	2.752e+8	6.064e+2	8.196
		std ₅₀	4.565e+11	3.713e+3	4.228
		CPU ₅₀	0.032	0.808	0.062
	MSE ₂₀₀	9.165e+12	3.399e+6	22.509	
	std ₂₀₀	2.459e+13	2.086e+7	6.103	
	CPU ₂₀₀	1.612	65.449	0.228	
	MSE ₄₀₀	8.423e+11	5.279e+2	31.589	
	std ₄₀₀	6.291e+12	1.288e+2	5.733	
	CPU ₄₀₀	4.087	128.800	0.230	

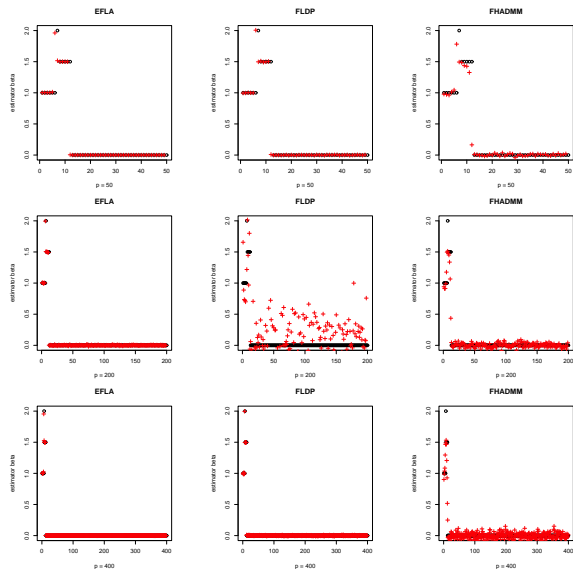


Fig. 1 The ground truth ‘o’ vs. the estimator ‘+’ under normal distribution error. The results with dimensions of $p = 50, 200$ and 400 are shown from top to bottom, and with methods of EFLA, FLDP, and FHADMM are shown from left to right

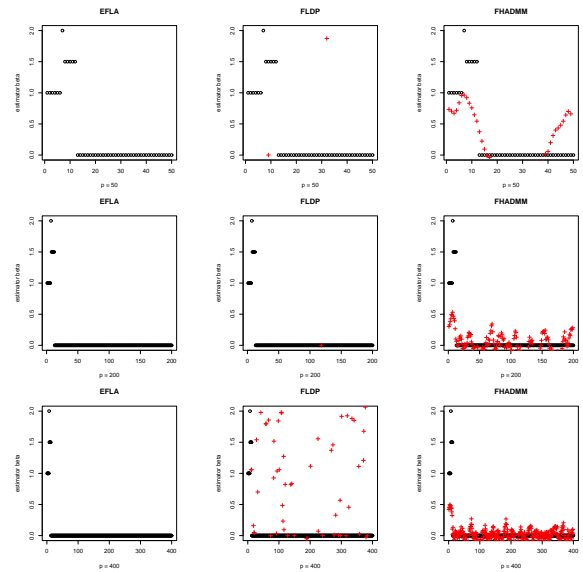


Fig. 3 The ground truth ‘o’ vs. the estimator ‘+’ under lognormal distribution error. The results with dimensions of $p = 50, 200$ and 400 are shown from top to bottom, and with methods of EFLA, FLDP, and FHADMM are shown from left to right

6 Numerical studies on real data

In this section, we further evaluate the effectiveness of our proposed estimation model and the progressiveness of the proposed algorithm FHADMM by using a triple of real datasets in the field of biology.

6.1 Leukemia Data

The Leukemia data was introduced by Golub et al. [30], which is available at the website: https://hastie.su.domains/CASL_files/DATA/leukemia.html. In this data set, there are 7129 genes and 72 samples where 47 in class 1 (acute lymphocytic leukemia) and 25 in class 2 (acute myelogenous leukemia). In order to explain how the gene expression level affects the biological function, we use 3707 genes among them.

The histogram of the kurtosis for these 3707 genes is shown in Figure 4. It shows that, there are 1980 out of 3707 gene expression variables have kurtosis larger than 3, and there are 213 out of 3707 larger than 9. In other words, there are more than 99.6% of the gene expression variables have tails heavier than the normal distribution,

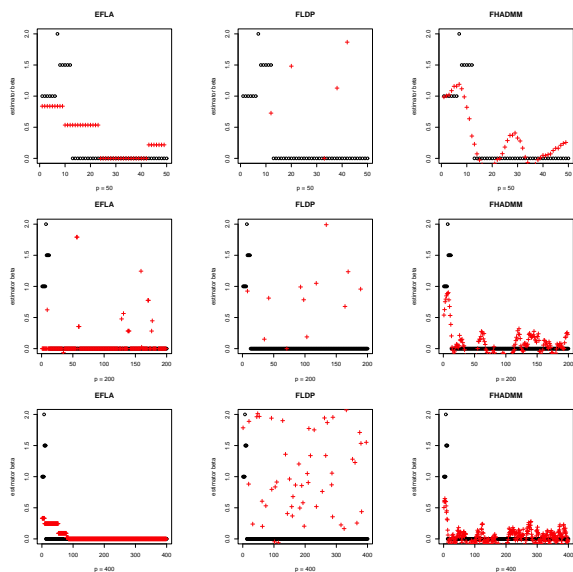


Fig. 2 The ground truth ‘o’ vs. the estimator ‘+’ under t distribution error. The results with dimensions of $p = 50, 200$ and 400 are shown from top to bottom, and with methods of EFLA, FLDP, and FHADMM are shown from left to right

and there are about 24.9% are severely heavy-tailed with tails flatter than the t distribution with degrees of freedom 5. This suggests that, the genomic data can still exhibit heavy tailedness regardless of any normalization methods, see Purdom & Holmes [31].

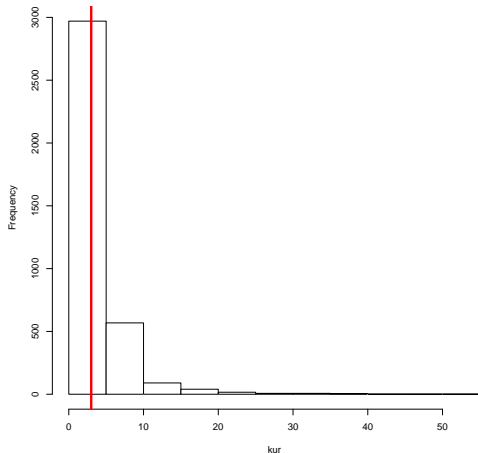


Fig. 4 Histogram of Kurtosises for the leukemia gene. The thick line at 3 is the kurtosis of a normal distribution

We should note that there are unordered features in our data set. Therefore, we apply hierarchical clustering to order the gene expression variables so as to exploring the property of fused lasso regularization. In this test, we divide the data set into a training data set with $n = 50$ and a test data set with $n_{test} = 22$. To measure the predictive accuracy, we use the robust prediction loss named Mean Absolute Error (MAE) in the form of

$$\text{MAE}(\hat{\beta}) := \frac{1}{n_{test}} \sum_{i=1}^{n_{test}} |y_i^{test} - \langle \mathbf{x}_i^{test}, \hat{\beta} \rangle|,$$

where y_i^{test} and \mathbf{x}_i^{test} , $i = 1, \dots, n_{test}$, coming from the test data set, respectively.

6.2 Liver Cancer Data

The Liver cancer data was given by Wheeler et al. [32] which is available at the website: <https://www.cancer.gov/about-nci/organization/ccg/research/structural-genomics/tcga>. In this data set, there are 19255 genes and 116 samples,

i.e., 58 in class 1 (patient) and 58 in class 2 (health). In order to find the genes with significant expression changes between their groups, we normalized the read-counts from the sequencing analysis. By using the R package DESeq2, we can obtain the DE result which contains $\log_2\text{FoldChange}$ and adjacent p-value. After filtering by specific thresholds, that is, $p_{adj} < 0.01$ and $|\log_2\text{FoldChange}| > 1.5$, it can be got that the number of genes with obvious difference is 2597.

The histograms about these 2597 genes of the kurtosises is displayed at the left hand side of Figure 5. It shows that, there are 709 out of 2597 gene expression variables have kurtosises larger than 3, and there are 239 out of 2597 larger than 9. Certainly, this data set also has heavy tailedness.

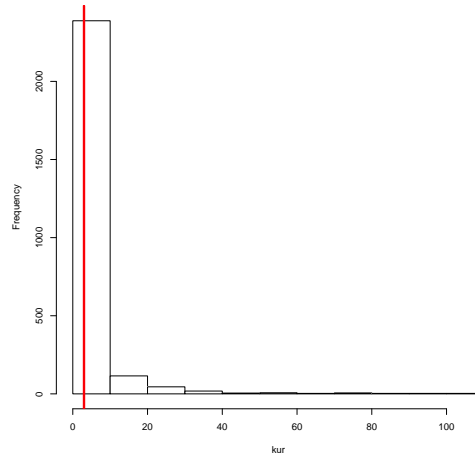


Fig. 5 Histogram of Kurtosises for the liver cancer gene. The thick line at 3 is the kurtosis of a normal distribution

As before, we also use the hierarchical clustering to order the gene expression variables in this data set. In this test, this data set is divided into a training data set with $n = 81$ and a test data set with $n_{test} = 35$. In addition, we also use the MAE to measure the algorithm's predictive performance.

6.3 Bladder Cancer Data

The Bladder cancer data was given in [33] which can be download at the website <https://www.cancer.gov/about-nci/organization/ccg/research/structural-genomics/tcga>. In this data set, there are 19211 genes and 40 samples:

21 in class 1 (patients) and 19 in class 2 (health). In a similar way, we can find that the number of genes with obvious difference is 2541. The histograms about these 2541 genes of the kurtosises of all expressions in the right hand side of Figure 6. It can be observed that, there are 2520 out of 2541 gene expression variables have kurtosises larger than 3, and there are 1494 gene expression variables larger than 9, which means that this data set is also heavy tailedness.

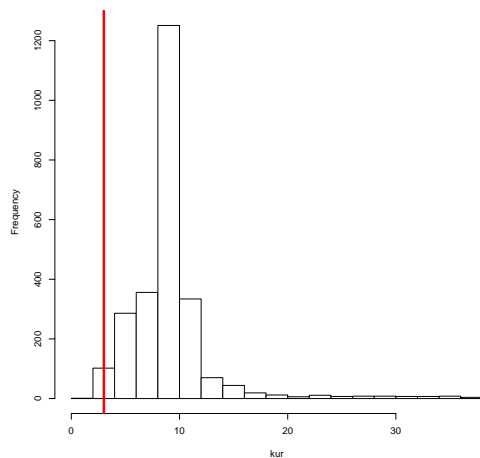


Fig. 6 Histogram of Kurtosises for the bladder cancer gene. The thick line at 3 is the kurtosis of a normal distribution

In addition, we also apply hierarchical clustering to order the gene expression variables, and partition this data set into a training data set with $n = 28$ and a test data set with $n_{test} = 12$.

6.4 Results' Comparisons

We run the methods EFLA, FLDP, and FHADMM by the using of the three types of real datasets viewed above, and report the MAE values in Table 2. From this table, we clearly observe that the MAE values derived by our proposed method FHADMM is the smallest, which is slightly smaller than the ones by FLDP and obviously smaller than the ones by EFLA. In summary, this simple table shows that the method FHADMM is the best but the FLDP is the worst.

To evaluate the benefit of the Huber function, we compare our fused lasso penalized adaptive Huber regression model (2) with the fused lasso

Table 2 The MAE values of EFLA, FLDP, and FHADMM on three types of data sets

methods	Leukemia	Liver	Bladder
EFLA	1.112	1.550	1.007
FLDP	0.944	5.029	0.960
FHADMM	0.928	0.998	0.779

penalized least square model, i.e., the Huber function term in (2) is replaced by a least square. The numerical results of the methods EFLA, FLDP, and FHADMM by using the real data set 'Leukemia', 'Liver', and 'Bladder' are report in Table 3, 4, and 5, respectively. In these tables, we only display the non-zero fragments of the derived coefficients by each method based on our fused lasso penalized huber model (2) and the fused lasso penalized least square model.

Comparing the values at the last column with the ones at the other columns, we see that, due to the influence of the coefficient difference constraint, it is preferable to scatter non-zero coefficients into the neighboring variables and obtain segmented smoothness solutions. While for the heavy tailedness, our model exhibits more robust than the model based on least square loss.

Table 3 Parts of estimated coefficients derived by each method on Leukemia data

No.	EFLA	FLDP	FHADMM
226	0.00000	0.00000	0.00066
227	0.00000	0.00000	0.00066
228	0.00000	0.00000	0.00066
516	0.00000	0.00000	0.00036
517	0.00000	0.02587	0.00036
771	0.00000	0.00000	0.00070
772	0.00000	0.00000	0.00070
774	0.00000	0.02194	0.00070
1808	0.06693	0.03654	0.00061
1809	0.00000	0.01689	0.00062
2053	0.00000	0.00000	0.00059
2054	0.00000	0.00000	0.00059
2109	0.01079	0.00000	0.00071
2110	0.01079	-0.00455	0.00071
2911	0.00000	0.00000	0.00096
2912	0.00000	0.00000	0.00096
3048	0.00000	0.00000	0.00051
3050	0.00000	0.00636	0.00051
3168	0.00000	-0.05059	-0.00024
3170	0.00000	0.00000	-0.00024

Table 4 Parts of estimated coefficients derived by each method on Liver data

No.	EFLA	FLDP	FHADMM
7	0.00000	-2.35199	0.00008
8	-2.48732	-2.38856	0.00008
108	0.00000	-1.26470	0.00002
109	0.00000	-1.26470	0.00002
121	0.00000	0.00000	0.00009
122	0.00000	0.00000	0.00009
173	0.00000	-3.69850	0.00008
174	0.00000	0.00000	0.00008
643	0.00000	0.97647	0.00002
644	0.00000	0.00000	0.00002
829	0.00000	0.00000	0.00003
830	0.00000	0.73268	0.00003
1090	-0.00002	0.00000	0.00003
1091	0.00000	0.00000	0.00003
2267	0.00000	-3.42318	0.00003
2268	0.00000	0.00000	0.00003
2498	0.00000	0.00000	0.00009
2499	0.00000	0.00000	0.00009
2500	0.00000	0.00000	0.00009
2501	0.00000	0.00000	0.00009

Table 5 Parts of estimated coefficients derived by each method on Bladder data

No.	EFLA	FLDP	FHADMM
5	0.00000	0.03337	0.00061
6	0.00000	0.03337	0.00061
125	0.00000	0.01287	0.00145
126	0.00000	0.01287	0.00145
163	0.00000	0.00000	0.00110
164	0.00000	0.00000	0.00110
212	0.00000	0.05537	0.00100
213	0.00000	0.03898	0.00100
220	0.00000	0.00167	0.00095
221	0.59375	0.00167	0.00095
651	0.00000	0.00000	0.00072
652	0.00000	0.02055	0.00072
1581	0.00000	0.00000	0.00075
1582	0.00000	0.06349	0.00075
2165	0.00000	0.00000	0.00055
2166	0.00000	0.00000	0.00055
2167	0.00000	0.00000	0.00055
2321	0.00000	0.00000	0.00056
2322	0.00000	0.00000	0.00056
2323	0.00000	0.00000	0.00056

7 Conclusion

In this paper, we focus on the fused lasso penalized adaptive Huber regression method. This method is widely used in many gene data sets because these datasets often have heavy tailedness and smoothness between adjacent genes. In

this paper, we studied the nonasymptotic property of this method and gave an upper bound with a higher probability. To implement this estimation method efficiently, we proposed an ADMM algorithm which has theoretical guarantees of global convergence in optimization literature. In simulation studies, we showed that our estimation method is very efficient in the t distribution noise case and the lognormal noise case. Especially, in a high-dimensional setting, our implemented algorithm FHADMM required less time than other state-of-the-art methods EFLA and FLDP.

At the end of this paper, it should be list some concluding remarks. Firstly, it should be noted that there are many modified Huber loss functions which can be considered to replace the standard Huber function in (2), such as smooth non-convex Huber[34], trimmed Huber[35] and so on. This should be an interesting topic for further research. Secondly, other related penalties, such as the sparse group fused lasso for model segmentation [3], also deserves further investigating. Thirdly, from the optimization theory, it is general known that numerical optimization algorithms based on dual problem may poss more nice properties for algorithms' design. Hence, some higher efficient optimization algorithms based on dual formulation is worthy of developing.

Acknowledges

This work of X. Xin is supported by Natural Science Foundation of Henan (Grant No. 202300410066). The work of Y. Xiao is supported by the National Natural Science Foundation of China (Grant No. 11971149).

Appendix A

A.1 Proof of Lemma 3.1

Proof First of all, we simply the notation $\mathbf{H}_\tau(\beta)$ as \mathbf{H}_τ by ignoring the variable β . Without loss of generality, we normalize each column of \mathbf{X} as $\|\mathbf{x}_i\|_\infty \leq 1$.

For any $(\mathbf{u}, \boldsymbol{\beta}) \in \mathcal{C}(m, c_0, r)$, we have

$$\begin{aligned}
& \langle \mathbf{u}, \mathbf{H}_\tau \mathbf{u} \rangle \\
&= \mathbf{u}^\top \left\{ \frac{1}{n} \sum_{i=1}^n \mathbf{x}_i \mathbf{x}_i^\top \mathbf{1}(|y_i - \langle \mathbf{x}_i, \boldsymbol{\beta} \rangle| \leq \tau) \right\} \mathbf{u} \\
&= \|\mathbf{S}_n^{1/2} \mathbf{u}\|_2^2 - \mathbf{u}^\top \left\{ \frac{1}{n} \sum_{i=1}^n \mathbf{x}_i \mathbf{x}_i^\top \mathbf{1}(|y_i - \langle \mathbf{x}_i, \boldsymbol{\beta} \rangle| > \tau) \right\} \mathbf{u} \\
&= \|\mathbf{S}_n^{1/2} \mathbf{u}\|_2^2 \\
&\quad - \mathbf{u}^\top \left\{ \frac{1}{n} \sum_{i=1}^n \mathbf{x}_i \mathbf{x}_i^\top \mathbf{1}(|y_i - \langle \mathbf{x}_i, \boldsymbol{\beta} - \boldsymbol{\beta}^* + \boldsymbol{\beta}^* \rangle| > \tau) \right\} \mathbf{u} \\
&\geq \|\mathbf{S}_n^{1/2} \mathbf{u}\|_2^2 - \frac{1}{n} \sum_{i=1}^n \langle \mathbf{u}, \mathbf{x}_i \rangle^2 \mathbf{1}(|\langle \mathbf{x}_i, \boldsymbol{\beta} - \boldsymbol{\beta}^* \rangle| \geq \tau/2) \\
&\quad - \frac{1}{n} \sum_{i=1}^n \langle \mathbf{u}, \mathbf{x}_i \rangle^2 \mathbf{1}(|\varepsilon_i| > \tau/2) \\
&\geq \|\mathbf{S}_n^{1/2} \mathbf{u}\|_2^2 - \frac{2r}{\tau} \|\mathbf{S}_n^{1/2} \mathbf{u}\|_2^2 \\
&\quad - \max_{1 \leq i \leq n} \langle \mathbf{u}, \mathbf{x}_i \rangle^2 \frac{1}{n} \sum_{i=1}^n \mathbf{1}(|\varepsilon_i| > \tau/2),
\end{aligned} \tag{A1}$$

where

$$\begin{aligned}
& \mathbf{1}(|\langle \mathbf{x}_i, \boldsymbol{\beta} - \boldsymbol{\beta}^* \rangle| \geq \tau/2) \\
&= \mathbf{1}\left(\frac{2}{\tau} |\langle \mathbf{x}_i, \boldsymbol{\beta} - \boldsymbol{\beta}^* \rangle| \geq 1\right) \\
&\leq \frac{2}{\tau} |\langle \mathbf{x}_i, \boldsymbol{\beta} - \boldsymbol{\beta}^* \rangle| \\
&\leq \frac{2}{\tau} \|\boldsymbol{\beta} - \boldsymbol{\beta}^*\|_1 \\
&\leq \frac{2r}{\tau}.
\end{aligned}$$

Without loss of generality, we consider the special case $\|\mathbf{u}_J\|_2^2 = 1$. Moreover, for any $1 \leq i \leq n$, by using Holder's inequality, we have that

$$\begin{aligned}
\langle \mathbf{u}, \mathbf{x}_i \rangle &\leq \|\mathbf{x}_i\|_\infty \|\mathbf{u}\|_1 \\
&\leq (1 + c_0) \|\mathbf{x}_i\|_\infty \|\mathbf{u}_J\|_1 \\
&\leq (1 + c_0) \sqrt{m} \|\mathbf{u}_J\|_2 = (1 + c_0) \sqrt{m}.
\end{aligned} \tag{A2}$$

In addition, for any $t > 0$ and $\tau > 0$, by using Markov's inequality, we have that

$$\begin{aligned}
& \mathbb{E}\left(\frac{1}{n} \sum_{i=1}^n \mathbf{1}(|\varepsilon_i| > \tau/2)\right) \\
&= \frac{1}{n} \sum_{i=1}^n P(|\varepsilon_i| > \tau/2) \\
&= \frac{1}{n} \sum_{i=1}^n P(|\varepsilon_i|^{1+\delta} > (\tau/2)^{1+\delta}) \\
&\leq v_\delta (2/\tau)^{1+\delta}.
\end{aligned}$$

Furthermore, applying Hoeffding's inequality, it yields, with probability at least $1 - e^{-t}$, that

$$\frac{1}{n} \sum_{i=1}^n \mathbf{1}(|\varepsilon_i| > \tau/2) \leq v_\delta (2/\tau)^{1+\delta} + \sqrt{t/(2n)}. \tag{A3}$$

Substituting (A2) and (A3) into (A1), we get

$$\begin{aligned}
& \langle \mathbf{u}, \mathbf{H}_\tau \mathbf{u} \rangle \\
&\geq \|\mathbf{S}_n^{1/2} \mathbf{u}\|_2^2 - \frac{2r}{\tau} \|\mathbf{S}_n^{1/2} \mathbf{u}\|_2^2 \\
&\quad - (1 + c_0)^2 m \left(v_\delta (2/\tau)^{1+\delta} + \sqrt{t/(2n)} \right).
\end{aligned}$$

Consequently, as long as $\tau \geq 8r$, we can get that the following inequality holds uniformly over $(\mathbf{u}, \boldsymbol{\beta}) \in \mathcal{C}(m, c_0, r)$ with probability at least $1 - e^{-t}$

$$\begin{aligned}
& \langle \mathbf{u}, \mathbf{H}_\tau \mathbf{u} \rangle \\
&\geq \frac{3}{4} \kappa_{low} - (1 + c_0)^2 m \left(v_\delta (2/\tau)^{1+\delta} + \sqrt{t/(2n)} \right) \\
&\geq \kappa_{low}/2,
\end{aligned} \tag{A4}$$

whenever

$$\tau \geq 2^{(4+\delta)/(1+\delta)} (1+c_0)^{2/(1+\delta)} \kappa_{low}^{-1/(1+\delta)} (mv_\delta)^{1/(1+\delta)}$$

and $n \geq 8(1 + c_0)^4 \kappa_{low}^{-2} m^2 t$. On the other hand, it is a easy task to prove that $\langle \mathbf{u}, \mathbf{H}_\tau \mathbf{u} \rangle \leq \kappa_{up}$. This completes the proof of the lemma. \square

A.2 Proof of Lemma 3.2

Proof Let $Q(l) := D_{\mathcal{L}}(\boldsymbol{\beta}_l, \boldsymbol{\beta}^*) := \mathcal{L}_\tau(\boldsymbol{\beta}_l) - \mathcal{L}_\tau(\boldsymbol{\beta}^*) - \langle \nabla \mathcal{L}_\tau(\boldsymbol{\beta}^*), \boldsymbol{\beta}_l - \boldsymbol{\beta}^* \rangle$. Then we have

$$Q'(l) = \langle \nabla \mathcal{L}_\tau(\boldsymbol{\beta}_l) - \nabla \mathcal{L}_\tau(\boldsymbol{\beta}^*), \boldsymbol{\beta} - \boldsymbol{\beta}^* \rangle.$$

Subsequently, the symmetric Bregman divergence $D_{\mathcal{L}}^s(\boldsymbol{\beta}_l, \boldsymbol{\beta}^*)$ can be rewritten equivalently as

$$\begin{aligned}
D_{\mathcal{L}}^s(\boldsymbol{\beta}_l, \boldsymbol{\beta}^*) &= \langle \nabla \mathcal{L}_\tau(\boldsymbol{\beta}_l) - \nabla \mathcal{L}_\tau(\boldsymbol{\beta}^*), l(\boldsymbol{\beta} - \boldsymbol{\beta}^*) \rangle \\
&= lQ'(l).
\end{aligned}$$

Setting $l = 1$, i.e., $D_{\mathcal{L}}^s(\boldsymbol{\beta}, \boldsymbol{\beta}^*) = Q'(1)$.

$Q(l)$ is convex because of the convexity of $\mathcal{L}_\tau(\boldsymbol{\beta}_l)$ and $\langle \nabla \mathcal{L}_\tau(\boldsymbol{\beta}^*), \boldsymbol{\beta}_l - \boldsymbol{\beta}^* \rangle$. Then its derivative $Q'(l)$ is non-decreasing, which also indicates that

$$D_{\mathcal{L}}^s(\boldsymbol{\beta}_l, \boldsymbol{\beta}^*) = lQ'(l) \leq lQ'(1) = lD_{\mathcal{L}}^s(\boldsymbol{\beta}, \boldsymbol{\beta}^*).$$

\square

A.3 Proof of Lemma 3.3

Proof Recalling that

$$D_{\mathcal{L}}^s(\boldsymbol{\beta}, \boldsymbol{\beta}^*) = \langle \nabla \mathcal{L}_\tau(\boldsymbol{\beta}) - \nabla \mathcal{L}_\tau(\boldsymbol{\beta}^*), \boldsymbol{\beta} - \boldsymbol{\beta}^* \rangle.$$

Denote $\boldsymbol{\Delta} := \boldsymbol{\beta} - \boldsymbol{\beta}^*$. By the mean value theorem, we have

$$D_{\mathcal{L}}^s(\boldsymbol{\beta}, \boldsymbol{\beta}^*) = \boldsymbol{\Delta}^\top \mathbf{H}_\tau(\tilde{\boldsymbol{\beta}}) \boldsymbol{\Delta},$$

where $\tilde{\beta}$ lies between β^* and β . Then we get

$$D_{\mathcal{L}}^s(\beta, \beta^*) \geq \lambda_{\min}(\mathbf{H}_{\tau}(\tilde{\beta})) \|\beta - \beta^*\|_2^2.$$

It remains to show that $\lambda_{\min}(\mathbf{H}_{\tau}(\tilde{\beta}))$ is lower bounded by a constant. There exists a $q \in [0, 1]$ such that $\tilde{\beta} = q\beta + (1-q)\beta^*$. Then it yields that

$$\|\tilde{\beta} - \beta^*\|_1 = q\|\beta - \beta^*\|_1 \leq qr,$$

which means that $\tilde{\beta} \in \mathcal{C}(m, c_0, r)$. By Lemma 3.1, we have $\lambda_{\min}(\mathbf{H}_{\tau}(\tilde{\beta})) \geq \frac{\kappa_{low}}{2}$ with probability $1 - e^{-t}$. Hence, we have

$$D_{\mathcal{L}}^s(\beta, \beta^*) \geq \frac{\kappa_{low}}{2} \|\beta - \beta^*\|_2^2.$$

□

A.4 Proof of Lemma 3.4

Proof From the first-order optimality condition, we know that there exist $\tilde{\omega}_1 \in \partial\|\hat{\beta}\|_1$ and $\tilde{\omega}_2 \in \partial\|\mathbf{D}\hat{\beta}\|_1$ such that

$$\nabla\mathcal{L}_{\tau}(\hat{\beta}) + \lambda_1\tilde{\omega}_1 + \lambda_2\tilde{\omega}_2 = 0. \quad (\text{A5})$$

From (5), we have

$$\langle \nabla\mathcal{L}_{\tau}(\hat{\beta}), \hat{\beta} - \beta^* \rangle \geq \langle \nabla\mathcal{L}_{\tau}(\beta^*), \hat{\beta} - \beta^* \rangle. \quad (\text{A6})$$

Substituting (A5) into (A6), we have

$$\begin{aligned} \langle \nabla\mathcal{L}_{\tau}(\beta^*), \hat{\beta} - \beta^* \rangle + \lambda_1 \langle \tilde{\omega}_1, \hat{\beta} - \beta^* \rangle \\ + \lambda_2 \langle \tilde{\omega}_2, \hat{\beta} - \beta^* \rangle \leq 0. \end{aligned} \quad (\text{A7})$$

For simplicity, we use I_1 , I_2 , and I_3 to denote the first, the second, and the third term at the left-hand-side of (A7). We now show their lower bound of I_1 , I_2 , and I_3 one by one.

(i) By Holder's inequality and the assumption that $\|\nabla\mathcal{L}_{\tau}(\beta^*)\|_{\infty} \leq \lambda_1/2$, we have

$$I_1 \geq -\|\nabla\mathcal{L}_{\tau}(\beta^*)\|_{\infty} \|\hat{\beta} - \beta^*\|_1 \geq -\lambda_1/2 \|\hat{\beta} - \beta^*\|_1. \quad (\text{A8})$$

(ii) From the subgradient of ℓ_1 -norm, we have $\|\hat{\beta}\|_1 = \langle \tilde{\omega}_1, \hat{\beta} \rangle$, and that $\|\tilde{\omega}_1\|_{\infty} \leq 1$. Furthermore, it also holds that

$$\begin{aligned} I_2 &= \lambda_1 \langle \tilde{\omega}_{1S}, (\hat{\beta} - \beta^*)_S \rangle + \lambda_1 \langle \tilde{\omega}_{1S^c}, (\hat{\beta} - \beta^*)_{S^c} \rangle \\ &\geq -\lambda_1 \|(\hat{\beta} - \beta^*)_S\|_1 + \lambda_1 \langle \tilde{\omega}_{1S^c}, (\hat{\beta} - \beta^*)_{S^c} \rangle \\ &\geq -\lambda_1 \|(\hat{\beta} - \beta^*)_S\|_1 + \lambda_1 \|(\hat{\beta} - \beta^*)_{S^c}\|_1, \end{aligned} \quad (\text{A9})$$

where the last inequality follows from the fact that $\langle \tilde{\omega}_{1S^c}, \hat{\beta}_{S^c} \rangle = \|\hat{\beta}_{S^c}\|_1$ and that $\beta_{S^c}^* = 0$.

(iii) In a similar way with (ii), we get $\|\mathbf{D}\hat{\beta}\|_1 = \langle \tilde{\omega}_2, \hat{\beta} \rangle$, and that $\|\tilde{\omega}_2\|_{\infty} \leq d$. Furthermore, we have

$$\begin{aligned} I_3 &= \lambda_2 \langle \tilde{\omega}_{2S}, (\hat{\beta} - \beta^*)_S \rangle + \lambda_2 \langle \tilde{\omega}_{2S^c}, (\hat{\beta} - \beta^*)_{S^c} \rangle \\ &\geq -\lambda_2 d \|(\hat{\beta} - \beta^*)_S\|_1 + \lambda_2 \langle \tilde{\omega}_{2S^c}, (\hat{\beta} - \beta^*)_{S^c} \rangle \\ &\geq -\lambda_2 d \|(\hat{\beta} - \beta^*)_S\|_1 + \lambda_2 d \|(\hat{\beta} - \beta^*)_{S^c}\|_1, \end{aligned} \quad (\text{A10})$$

where the last inequality follows from the fact that $\langle \tilde{\omega}_{2S^c}, \mathbf{D}\hat{\beta}_{S^c} \rangle = \|\mathbf{D}\hat{\beta}_{S^c}\|_1 = d\|\hat{\beta}_{S^c}\|_1$ and that $\beta_{S^c}^* = 0$.

Substituting (A8), (A9), and (A10) into (A7), we get

$$\begin{aligned} -\lambda_1/2 \|\hat{\beta} - \beta^*\|_1 - \lambda_1 \|(\hat{\beta} - \beta^*)_S\|_1 + \lambda_1 \|(\hat{\beta} - \beta^*)_{S^c}\|_1 \\ - \lambda_2 d \|(\hat{\beta} - \beta^*)_S\|_1 + \lambda_2 d \|(\hat{\beta} - \beta^*)_{S^c}\|_1 \leq 0, \end{aligned}$$

or equivalently,

$$\|(\hat{\beta} - \beta^*)_{S^c}\|_1 \leq \frac{2bd+3}{2bd+1} \|(\hat{\beta} - \beta^*)_S\|_1.$$

□

A.5 Proof of Theorem 1

Proof Using the first-order optimality condition as same as (A5), and substituting (A5) into (5), we have

$$\begin{aligned} D_{\mathcal{L}}^s(\hat{\beta}, \beta^*) &= \langle -\nabla\mathcal{L}_{\tau}(\beta^*) - \lambda_1\tilde{\omega}_1 - \lambda_2\tilde{\omega}_2, \hat{\beta} - \beta^* \rangle \\ &= \langle \nabla\mathcal{L}_{\tau}(\beta^*), \beta^* - \hat{\beta} \rangle + \lambda_1 \langle \tilde{\omega}_1, \beta^* - \hat{\beta} \rangle \\ &\quad + \lambda_2 \langle \tilde{\omega}_2, \beta^* - \hat{\beta} \rangle. \end{aligned} \quad (\text{A11})$$

Once again, for the sake of simplicity, we denote the right-hand-side terms at (A11) as I_1 , I_2 , and I_3 , respectively, and then turn our attention to their upper bounds.

(i) By Holder's inequality and Lemma 3.4, we have

$$\begin{aligned} I_1 &\leq \|\nabla\mathcal{L}_{\tau}(\beta^*)\|_{\infty} \|\hat{\beta} - \beta^*\|_1 \leq \frac{\lambda_1}{2} \|\hat{\beta} - \beta^*\|_1 \\ &= \frac{\lambda_1}{2} \left(\|(\hat{\beta} - \beta^*)_S\|_1 + \|(\hat{\beta} - \beta^*)_{S^c}\|_1 \right) \\ &\leq \frac{2\lambda_1(bd+1)}{2bd+1} \|(\hat{\beta} - \beta^*)_S\|_1. \end{aligned} \quad (\text{A12})$$

(ii) Using Holder's inequality and Lemma 3.4 again, we get

$$\begin{aligned} I_2 &\leq \lambda_1 \|\tilde{\omega}_1\|_{\infty} \|\hat{\beta} - \beta^*\|_1 \leq \lambda_1 \|\hat{\beta} - \beta^*\|_1 \\ &= \lambda_1 \left(\|(\hat{\beta} - \beta^*)_S\|_1 + \|(\hat{\beta} - \beta^*)_{S^c}\|_1 \right) \\ &\leq \frac{4\lambda_1(bd+1)}{2bd+1} \|(\hat{\beta} - \beta^*)_S\|_1. \end{aligned} \quad (\text{A13})$$

(iii) For I_3 , we have

$$\begin{aligned} I_3 &\leq \lambda_2 \|\tilde{\omega}_2\|_{\infty} \|\hat{\beta} - \beta^*\|_1 \leq \lambda_2 d \|\hat{\beta} - \beta^*\|_1 \\ &= \lambda_2 d \left(\|(\hat{\beta} - \beta^*)_S\|_1 + \|(\hat{\beta} - \beta^*)_{S^c}\|_1 \right) \\ &\leq \frac{4\lambda_2 d(bd+1)}{2bd+1} \|(\hat{\beta} - \beta^*)_S\|_1. \end{aligned} \quad (\text{A14})$$

Substituting (A12), (A13) and (A14) into (A11), it yields that

$$\begin{aligned} D_{\mathcal{L}}^s(\hat{\beta}, \beta^*) &\leq \frac{2\lambda_1(2bd+3)(bd+1)}{2bd+1} \|(\hat{\beta} - \beta^*)_S\|_1 \\ &\leq \frac{2\lambda_1(2bd+3)(bd+1)}{2bd+1} \sqrt{s} \|(\hat{\beta} - \beta^*)_S\|_2, \end{aligned} \quad (\text{A15})$$

where $s = |\text{supp}(\beta^*)|$ is a sparsity parameter.

In what follows, we employ Lemma 3.3 to obtain a lower bound for the symmetric Bregman divergence. At the first place, we denote $\hat{\beta}_l := \beta^* + l(\hat{\beta} - \beta^*)$, $l \in (0, 1]$ such that $\|\hat{\beta}_l - \beta^*\|_1 \leq r$ for some $r > 0$.

In fact, if $\|\hat{\beta} - \beta^*\|_1 < r$, we can set $l = 1$ which means that $\hat{\beta}_l = \hat{\beta}$ and $\|\hat{\beta}_l - \beta^*\|_1 < r$; otherwise if $\|\hat{\beta} - \beta^*\|_1 \geq r$, we choose $l \in (0, 1)$ such that $\|\hat{\beta}_l - \beta^*\|_1 = r$.

Hence, $\hat{\beta}_l$ falls into a local ℓ_1 cone, i.e., $\hat{\beta}_l \in \mathcal{C}(m, c_0, r)$. Then by Lemma 3.4,

$$\|(\hat{\beta}_l - \beta^*)_{S^c}\|_1 \leq \frac{2bd + 3}{2bd + 1} \|(\hat{\beta}_l - \beta^*)_S\|_1. \quad (\text{A16})$$

Then by Lemma 3.3, we have

$$D_{\mathcal{L}}^s(\hat{\beta}_l, \beta^*) \geq \frac{\kappa_{low}}{2} \|\hat{\beta}_l - \beta^*\|_2^2. \quad (\text{A17})$$

By Lemma 3.2, we have

$$D_{\mathcal{L}}^s(\hat{\beta}_l, \beta^*) \leq l D_{\mathcal{L}}^s(\hat{\beta}, \beta^*). \quad (\text{A18})$$

Combining (A17) and (A18) with (A15), it yields that

$$\|\hat{\beta}_l - \beta^*\|_2^2 \leq \frac{4\lambda_1(2bd + 3)(bd + 1)}{2bd + 1} \kappa_{low}^{-1} l \sqrt{s} \|\hat{\beta} - \beta^*\|_2.$$

Because $\hat{\beta} - \beta^* = l^{-1}(\hat{\beta}_l - \beta^*)$, we have

$$\begin{aligned} \|\hat{\beta}_l - \beta^*\|_2 &\leq \frac{4\lambda_1(2bd + 3)(bd + 1)}{2bd + 1} \kappa_{low}^{-1} \sqrt{s} \\ &\leq \frac{4\lambda_1(2bd + 3)(bd + 1)}{2bd + 1} \kappa_{low}^{-1} \sqrt{s}. \end{aligned}$$

Finally, by (A16), we have

$$\begin{aligned} \|\hat{\beta}_l - \beta^*\|_1 &\leq \frac{4(bd + 1)}{2bd + 1} \sqrt{s} \|(\hat{\beta}_l - \beta^*)\|_2 \\ &\leq \frac{16\lambda_1(bd + 1)^2(2bd + 3)}{(2bd + 1)^2} \kappa_{low}^{-1} s < r, \end{aligned}$$

where the last inequality is from the assumption that $r \gtrsim \lambda_1 \kappa_{low}^{-1} s$ and $n \geq c_3 m^2 t$ for a sufficiently large constant $c_3 > 0$. Because $\|\hat{\beta}_l - \beta^*\|_1 < r$, we have $\hat{\beta}_l = \hat{\beta}$, which means that

$$\|\hat{\beta} - \beta^*\|_2 \leq \frac{4\lambda_1(2bd + 3)(bd + 1)}{2bd + 1} \kappa_{low}^{-1} \sqrt{s} \quad (\text{A19})$$

holds with probability at least $1 - e^{-t}$.

It remains to bound the probability so that the required condition $\|\nabla \mathcal{L}_\tau(\beta^*)\|_\infty \leq \lambda_1/2$ in Lemma 3.4 holds. Following the argument used in the proof of Sun et al. [11, Theorem 1], we take $\tau := \tau_0(n/t)^{1/(1+\delta)}$ for some $\tau_0 \geq \nu_\delta$ and reach

$$P\{\|\nabla \mathcal{L}_\tau(\beta^*)\|_\infty \geq 2\tau t/n\} \leq 2pe^{-t}.$$

Hence, we have $\lambda_1/2 \geq 2\tau t/n$, that is $\lambda_1 \geq 4\tau_0(t/n)^{\delta/(1+\delta)}$. Then, together with (A19), we can prove that

$$\|\hat{\beta} - \beta^*\|_2 \leq \lambda_1 \kappa_{low}^{-1} \sqrt{s}$$

holds with probability at least $1 - (1 + 2p)e^{-t}$. \square

References

- [1] Li, X., Sun, D., Toh, K.-C.: On efficiently solving the subproblems of a level-set method for fused lasso problems. *SIAM Journal on Optimization* **28**(2), 1842–1866 (2018)
- [2] Li, M., Guo, Q., Zhai, W., Chen, B.: The linearized alternating direction method of multipliers for low-rank and fused lasso matrix regression model. *Journal of Applied Statistics* **47**(13-15), 2623–2640 (2020)
- [3] Degras, D.: Sparse group fused lasso for model segmentation: a hybrid approach. *Advances in Data Analysis and Classification* **15**(3), 625–671 (2021)
- [4] Tibshirani, R., Saunders, M., Rosset, S., Zhu, J., Knight, K.: Sparsity and smoothness via the fused lasso. *Journal of the Royal Statistical Society: Series B (Statistical Methodology)* **67**(1), 91–108 (2005)
- [5] Petersen, A., Witten, D., Simon, N.: Fused lasso additive model. *Journal of Computational and Graphical Statistics* **25**(4), 1005–1025 (2016)
- [6] Mao, R., Chen, Z., Hu, G.: Robust temporal low-rank representation for traffic data recovery via fused lasso. *IET Intelligent Transport Systems* **15**(2), 175–186 (2021)
- [7] Corsaro, S., De Simone, V., Marino, Z.: Fused lasso approach in portfolio selection. *Annals of Operations Research* **299**(1), 47–59 (2021)
- [8] Cui, L., Bai, L., Wang, Y., Philip, S.Y., Hancock, E.R.: Fused lasso for feature selection using structural information. *Pattern Recognition* **119**, 108058 (2021)
- [9] Li, X., Mo, L., Yuan, X., Zhang, J.: Linearized alternating direction method of multipliers for sparse group and fused lasso models. *Computational Statistics & Data Analysis* **79**, 203–221 (2014)
- [10] Wang, F., Wang, L., Song, P.X.-K.: Fused lasso with the adaptation of parameter ordering in combining multiple studies with

- repeated measurements. *Biometrics* **72**(4), 1184–1193 (2016)
- [11] Sun, Q., Zhou, W.-X., Fan, J.: Adaptive huber regression. *Journal of the American Statistical Association* **115**(529), 254–265 (2020)
- [12] Huang, S., Wu, Q.: Robust pairwise learning with huber loss. *Journal of Complexity* **66**, 101570 (2021)
- [13] Liu, Y., Zeng, P., Lin, L.: Degrees of freedom for regularized regression with huber loss and linear constraints. *Statistical Papers* **62**(5), 2383–2405 (2021)
- [14] Fan, J., Liu, H., Sun, Q., Zhang, T.: I-lamm for sparse learning: Simultaneous control of algorithmic complexity and statistical error. *Annals of statistics* **46**(2), 814 (2018)
- [15] Chen, B., Zhai, W., Huang, Z.: Low-rank elastic-net regularized multivariate huber regression model. *Applied Mathematical Modelling* **87**, 571–583 (2020)
- [16] Luo, J., Sun, Q., Zhou, W.-X.: Distributed adaptive huber regression. *Computational Statistics & Data Analysis* **169**, 107419 (2022)
- [17] Ghosh, D., Kaabouch, N., Hu, W.-C.: A robust iterative super-resolution mosaicking algorithm using an adaptive and directional huber-markov regularization. *Journal of Visual Communication and Image Representation* **40**, 98–110 (2016)
- [18] Xiao, Y., Wu, S.-Y., Li, D.-H.: Splitting and linearizing augmented lagrangian algorithm for subspace recovery from corrupted observations. *Advances in Computational Mathematics* **38**(4), 837–858 (2013)
- [19] Jiao, Y., Jin, Q., Lu, X., Wang, W.: Alternating direction method of multipliers for linear inverse problems. *SIAM Journal on Numerical Analysis* **54**(4), 2114–2137 (2016)
- [20] Huber, P.: *Robust statistics*. Wiley, New York (1981)
- [21] Rockafellar, R.T.: *Convex Analysis*. Princeton university press, Princeton (1970)
- [22] Bonnans, J.F., Shapiro, A.: *Perturbation Analysis of Optimization Problems*. Springer, New York (2013)
- [23] Boyd, S., Parikh, N., Chu, E., Peleato, B., Eckstein, J., *et al.*: Distributed optimization and statistical learning via the alternating direction method of multipliers. *Foundations and Trends® in Machine learning* **3**(1), 1–122 (2011)
- [24] Fazel, M., Pong, T.K., Sun, D., Tseng, P.: Hankel matrix rank minimization with applications to system identification and realization. *SIAM Journal on Matrix Analysis and Applications* **34**(3), 946–977 (2013)
- [25] Yang, W.H., Han, D.: Linear convergence of the alternating direction method of multipliers for a class of convex optimization problems. *SIAM journal on Numerical Analysis* **54**(2), 625–640 (2016)
- [26] Wang, H., Li, R., Tsai, C.-L.: Tuning parameter selectors for the smoothly clipped absolute deviation method. *Biometrika* **94**(3), 553–568 (2007)
- [27] Jiao, Y., Jin, B., Lu, X.: A primal dual active set with continuation algorithm for the ℓ_0 -regularized optimization problem. *Applied and Computational Harmonic Analysis* **39**(3), 400–426 (2015)
- [28] Liu, J., Yuan, L., Ye, J.: An efficient algorithm for a class of fused lasso problems. In: *Proceedings of the 16th ACM SIGKDD International Conference on Knowledge Discovery and Data Mining*, pp. 323–332 (2010)
- [29] Tibshirani, R.J., Taylor, J.: The solution path of the generalized lasso. *The annals of statistics* **39**(3), 1335–1371 (2011)
- [30] Golub, T.R., Slonim, D.K., Tamayo, P., Huard, C., Gaasenbeek, M., Mesirov, J.P., Coller, H., Loh, M.L., Downing, J.R., Caligiuri, M.A., *et al.*: Molecular classification of cancer: class discovery and class

prediction by gene expression monitoring. *science* **286**(5439), 531–537 (1999)

- [31] Elizabeth, P., *et al.*: Error distribution for gene expression data. *Statistical Applications in Genetics and Molecular Biology* **4**(1), 1–35 (2005)
- [32] Wheeler, D.A., Roberts, L.R., Network, C.G.A.R., *et al.*: Comprehensive and integrative genomic characterization of hepatocellular carcinoma. *Cell* **169**(7), 1327 (2017)
- [33] Network, C.G.A.R., *et al.*: Comprehensive molecular characterization of urothelial bladder carcinoma. *Nature* **507**(7492), 315 (2014)
- [34] Zhong, P.: Training robust support vector regression with smooth non-convex loss function. *Optimization Methods and Software* **27**, 1039–1058 (2012)
- [35] Chen, C., Yan, C., Zhao, N., Guo, B., Liu, G.: A robust algorithm of support vector regression with a trimmed huber loss function in the primal. *Soft Computing* **21**(18), 5235–5243 (2017)